

A two patch prey-predator model with multiple foraging strategies in predators: Applications to Insects

Komi Messan^a, Yun Kang^b

^a*Simon A. Levin Mathematical and Computational Modeling Sciences Center, Arizona State University, Tempe, AZ 85281, USA.*

^b*Sciences and Mathematics Faculty, College of Letters and Sciences, Arizona State University, Mesa, AZ 85212, USA.*

Abstract

We propose and study a two patch Rosenzweig-MacArthur prey-predator model with immobile prey and predator using two dispersal strategies. The first dispersal strategy is driven by the prey-predator interaction strength, and the second dispersal is prompted by the local population density of predators which is referred as the passive dispersal. The dispersal strategies using by predator are measured by the proportion of the predator population using the passive dispersal strategy which is a parameter ranging from 0 to 1. We focus on how the dispersal strategies and the related dispersal strengths affect population dynamics of prey and predator, hence generate different spatial dynamical patterns in heterogeneous environment. We provide local and global dynamics of the proposed model. Based on our analytical and numerical analysis, interesting findings could be summarized as follow: (1) If there is no prey in one patch, then the large value of dispersal strength and the large predator population using the passive dispersal in the other patch could drive predator extinct at least locally. However, the intermediate predator population using the passive dispersal could lead to multiple interior equilibria and potentially stabilize the dynamics; (2) The large dispersal strength in one patch may stabilize the boundary equilibrium and lead to the extinction of predator in two patches locally when predators use two dispersal strategies; (3) For symmetric patches (i.e., all the life history parameters are the same except the dispersal strengths), the large predator population using the passive dispersal can generate multiple interior attractors; (4) The dispersal strategies can stabilize the system, or destabilize the system through generating multiple interior equilibria that lead to multiple attractors; and (5) The large predator population using the passive dispersal could lead to no interior equilibrium but both prey and predator can coexist through fluctuating dynamics for almost all initial conditions.

Keywords: The Rosenzweig-MacArthur prey-predator Model; Dispersal strategies; Predation strength; Passive dispersal

Email addresses: kmessan@asu.edu (Komi Messan), yun.kang@asu.edu (Yun Kang)

1. Introduction

The dispersal of an individual has consequences not only for individual fitness, but also for population dynamics and genetics, and species' distributions (Bowler and Benton, 2005; Clobert et al., 2001; Gilpin and Hanski, 1991; Hanski, 1999). As the impact of dispersal on population dynamics has been increasingly recognized, understanding the link between dispersal and population dynamics is vital for population management and for predicting how population responses to changes in the environment. For many animals and insects, the costs and benefits of dispersal will vary in space and time, and among individuals. Thus, the profit of the dispersal ability as a life-history strategy will vary as a result, and a plastic dispersal strategy is typically expected to respond to this variation (Bowler and Benton, 2005; Ims and Hjermann, 2001; Massot et al., 2002; Ronce et al., 2001). The varied dispersal driving forces include population density, kin selection relatedness, conspecific attraction, interspecific interactions, food availability, patch size and qualities, etc. There has been a large number of empirical studies supporting the effects of various parameters on dispersal mechanisms and strengths (Bowler and Benton, 2005). For example, the field work by Kiester and Slatkin (1974) showed evidence of Iguanid lizards that encompass two or more dispersal strategies as foraging movements. Kummel et al. (2013) showed through their field work that the foraging behavior of Coccinellids are governed not only by the conspecific attraction but also through the passive diffusion and retention on plants with high immobile aphids number. The main purpose of this article is to investigate the effects of the combinations of different strategies on population dynamics of a prey-predator interaction model when prey is immobile.

Due to the practical difficulties associated with the field study of dispersal, theoretical studies play a particularly important role in predicting the effects of varied dispersal strategies in population dynamics (Bowler and Benton, 2005). The patchy prey-predator population models with different dispersal forms have been proposed and studied in a fair amount of literature. For example, the work of (Fraser and Cerri, 1982; Hansson, 1991; János and Scheuring, 1997; Namba, 1980; Nguyen-Ngoc et al., 2012; Savino and Stein, 1989; Silva et al., 2001) explored the effects of dispersal on population dynamics of prey-predator models when local population density is a selecting factor for dispersal. The work of Huang and Diekmann (2001) and Ghosh and Bhattacharyya (2011) studied the population dynamics of a two patch model with dispersal in predator driving by local population density of prey through Holling searching-handling time budget argument. The work of Kareiva and Odell (1987) studied dynamics when the dispersal of predator is carried out due to the concentrated food resources. Cressman and Křivan (2013) investigated a two patch population-dispersal dynamics for predator-prey interactions with dispersal directed by the fitness. Recent work of (Kang et al., 2014) studied a two patch prey-predator model where predator is dispersed to the patch with the stronger strength of prey-predator interaction. These theoretical work provide useful insights on the link of dispersal strategies and prey-predator population dynamics.

Many empirical work of animal and insects show that dispersal strategies vary among species according to their life history and how they interact with the environment (Bowler and Benton, 2005). However, there is a limited theoretical work on studying how combinations of different dispersal strategies affect population dynamics of prey-predator models in the patchy environment. This paper presents an extended version of a Rosenzweig-MacArthur two patch prey-predator model studied in (Kang et al., 2014) where prey is immobile and the dispersal of predator is attracted

by the strength of prey-predation interaction. Our proposed model is motivated by the field experiments of (Kiestler and Slatkin, 1974; Kummel et al., 2013; Stamps, 1988). The current model integrates the two dispersal strategies of predator: (1) the passive dispersal, i.e., the classical foraging behavior where predator is driven to the patch with the lower predator population density (e.g. (Jansen, 1995)); (2) the density dependent dispersal measured through the predation attraction (Kang et al., 2014). The linear combination of these two strategies is linked through a parameter whose value is between 0 and 1, and measures the proportion of the predator population using these two dispersal strategies. We aim to use our model to explore how the combinations of these two dispersal strategies of predator affect population dynamics of prey-predator interaction.

The paper is organized as follows: Section 2 introduces the proposed model along with its biological derivation, and provide a brief summary on the dynamics of the related subsystems. Section 3 presents mathematical analysis of the local and global dynamics of the proposed model. Section 4 Investigates the effects of dispersal strategies through bifurcation diagrams. Section 5 concludes our findings along with the related potential biological interpretations.

2. Model derivations and the related dynamics

Let $x_i(t)$, $y_i(t)$ be the population of prey and predator in Patch i at time t , respectively. In the absence of dispersal, we assume that the population dynamics of prey and predator follow the Rosenzweig-MacArthur prey-predator model. The dispersal of predator from Patch i to Patch j is driven by two mechanisms. The first mechanism relies on the strength of the prey-predation interaction in Patch j (also called “the predation strength”). Let ρ_i represents the relative dispersal rate of predator at Patch i , then we obtained the following net predation attraction driven dispersal of predator at Patch i

$$\rho_i \left(\frac{a_j x_j y_j}{1 + x_j} y_i - \frac{a_i x_i y_i}{1 + x_i} y_j \right).$$

This assumption follows directly from the experimental work of Stamps (1988) in which he concluded that *Anolis aeneus* juveniles are attracted to conspecific territorial residents under natural conditions in the field. This assumption has also been supported by many field studies including (Alonso et al., 2004; Auger and Poggiale, 1996; Hassell and Southwood, 1978).

The second dispersal mechanism is termed as “the passive dispersal” in which the dispersal is driven by the local population density of predator. The effects of this dispersal strategy has been well studied by many researchers (Hastings, 1983; János and Scheuring, 1997; Jansen, 1995; Matthysen, 2005; Namba, 1980; Nguyen-Ngoc et al., 2012; Poggiale, 1998; Silva et al., 2001). For example overcrowding of predator in a patch may decrease the resource assessment that can constitute a cue for for the local predators to move. Following this inference, the net dispersal of predators from Patch i to Patch j is given by

$$\rho_i (y_j - y_i).$$

Motivated by the field work of Kiestler and Slatkin (1974) on Iguanid lizards and Kummel et al. (2013) on Coccinellids, we incorporate these two dispersal strategies above into our model. After

similar rescaling approach by [Liu and Chen \(2003\)](#), our proposed model is presented as follows with $r_1 = 1, r_2 = r$ being the relative intrinsic growth rates, K_i being the relative carrying capacity of prey at Patch i in the absence of predation, d_i being the death rate of predator in Patch i , and the parameter $s \in [0, 1]$ representing the proportion of predator population using the passive dispersal strategy:

$$\begin{aligned}
\frac{dx_1}{dt} &= r_1 x_1 \left(1 - \frac{x_1}{K_1}\right) - \frac{a_1 x_1 y_1}{1 + x_1} \\
\frac{dy_1}{dt} &= \frac{a_1 x_1 y_1}{1 + x_1} - d_1 y_1 + \rho_1 (1 - s) \left(\underbrace{\frac{a_1 x_1 y_1}{1 + x_1}}_{\text{attraction strength to Patch 1}} y_2 - \underbrace{\frac{a_2 x_2 y_2}{1 + x_2}}_{\text{attraction strength to Patch 2}} y_1 \right) + \rho_1 s (y_2 - y_1) \\
\frac{dx_2}{dt} &= r_2 x_2 \left(1 - \frac{x_2}{K_2}\right) - \frac{a_2 x_2 y_2}{1 + x_2} \\
\frac{dy_2}{dt} &= \frac{a_2 x_2 y_2}{1 + x_2} - d_2 y_2 + \rho_2 (1 - s) \left(\underbrace{\frac{a_2 x_2 y_2}{1 + x_2}}_{\text{attraction strength to Patch 2}} y_1 - \underbrace{\frac{a_1 x_1 y_1}{1 + x_1}}_{\text{attraction strength to Patch 1}} y_2 \right) + \rho_2 s (y_1 - y_2)
\end{aligned} \tag{1}$$

First, we have the following theorem regarding the basic dynamic properties of Model (1):

Theorem 2.1. *Assume that all parameters are positive. Model (1) is positively invariant and bounded in \mathbb{R}_+^4 . In addition, the set $\{(x_1, y_1, x_2, y_2) \in \mathbb{R}_+^4 : x_i = 0\}$ is invariant for both $i = 1, 2$.*

Our main focus is to explore how the combination of two different dispersal strategies measured by the parameter $s \in [0, 1]$ affect the two patch population dynamics. Before we continue, we first provide a summary of the dynamics of the subsystems of Model (1) including the cases of $s = 0$ and $s = 1$.

For convenience, let $\mu_i = \frac{d_i}{a_i - d_i}$, and $\nu_i = \frac{r_i(K_i - \mu_i)(1 + \mu_i)}{a_i K_i}$ $i = 1, 2$, then in the absence of dispersal in predator, Model (1) is reduced to the following [Rosenzweig and MacArthur \(1963\)](#) prey-predator single patch models $i = 1, 2$

$$\begin{aligned}
\frac{dx_i}{dt} &= r_i x_i \left(1 - \frac{x_i}{K_i}\right) - \frac{a_i x_i y_i}{1 + x_i} \\
\frac{dy_i}{dt} &= \frac{a_i x_i y_i}{1 + x_i} - d_i y_i
\end{aligned} \tag{2}$$

with $r_1 = 1$ and $r_2 = r$ and its global dynamics which can be summarized from the work of ([Hsu et al., 1977](#); [Hsu, 1978](#); [Liu and Chen, 2003](#)) as follows:

1. Model (2) always has two boundary equilibria $(0, 0)$, $(K_i, 0)$ where the extinction $(0, 0)$ is always a saddle.
2. The boundary equilibria $(K_i, 0)$ is globally asymptotically stable if $\mu_i > K_i$.
3. If $\frac{K_i - 1}{2} < \mu_i < K_i$, then $(K_i, 0)$ becomes saddle and the unique interior equilibria (μ_i, ν_i) emerges which is globally asymptotically stable.

4. If $0 < \mu_i < \frac{K_i-1}{2}$, the boundary equilibrium $(K_i, 0)$ is a saddle, and the unique interior equilibrium (μ_i, ν_i) is a source where Hopf bifurcation occurs at $\mu_i = \frac{K_i-1}{2}$. The system (2) has a unique stable limit cycle.

The summary on the dynamics of Model (1) when the dispersal of predator foraging activities is driven by local population density (i.e., $s = 1$) and when the dispersal of predator foraging activities is driven by predation strength (i.e. $s = 0$) are briefly presented in Table 3 (see Kang et al. (2014) for more detailed summary on the global dynamics).

3. Mathematical analysis

From Theorem 2.1, we know that the set $\{(x_1, y_1, x_2, y_2) \in \mathbb{R}_+^4 : x_i = 0\}$, is invariant for both $i = 1, 2$. Assume that $x_j = 0$, Model (1) is reduced to the following three species subsystem:

$$\begin{aligned}\frac{dx_i}{dt} &= r_i x_i \left(1 - \frac{x_i}{K_i}\right) - \frac{a_i x_i y_i}{1 + x_i} \\ \frac{dy_i}{dt} &= \frac{a_i x_i y_i}{1 + x_i} - d_i y_i + \rho_i (1 - s) \left(\frac{a_i x_i y_i}{1 + x_i} y_j\right) + \rho_i s (y_j - y_i) \\ \frac{dy_j}{dt} &= -d_j y_j - \rho_j (1 - s) \left(\frac{a_i x_i y_i}{1 + x_i} y_j\right) - \rho_j s (y_j - y_i)\end{aligned}\tag{3}$$

whose basic dynamics are provided in the following theorem:

Theorem 3.1. *[Basic dynamics of Model (3)] Let $\mu_i = \frac{d_i}{a_i - d_i}$ and $s \in (0, 1)$, then the following statements of Model (3) are held:*

1. Prey x_i is persistent with $\limsup_{t \rightarrow \infty} x_i(t) \leq K_i$.
2. If $\mu_i > K_i$, then predators in two patches go extinct, and the system (3) has global stability at $(K_i, 0, 0)$.
3. If $\rho_i s < \frac{(a_i - d_i)(K_i - \mu_i)}{1 + K_i}$, then predators in the two patches are persistent.

Notes: Model (3) can apply to the case where Patch i is the source patch with prey population and Patch j is the sink patch without prey population. The predator in the sink patch is migrated from the source patch. Theorem 3.1 indicates the follows regarding the effects of the proportion of predator using the passive dispersal on Model (3):

1. Prey x_i of Model (3) is always persistent for all $r_i > 0$. This is different than the case of $s = 1$ since prey may go extinct when $s = 1$.
2. If $\mu_i < K_i$ and $\rho_i s$ is small enough, then the inequality $\rho_i s < \frac{(a_i - d_i)(K_i - \mu_i)}{1 + K_i}$ holds, hence predators persist. This result suggests that, under the condition of $\mu_i < K_i$, the large value of $\rho_i s$ could drive predator extinction in two patches at least locally.

The interior equilibria (x_1^*, y_1^*, y_2^*) of Model (3) is determined by first solving for y_i^* and x_i^* in $\frac{dx_i}{dt} = 0$ and $\frac{dy_j}{dt} = 0$ as follows:

$$\begin{aligned} \frac{dx_i}{dt} = 0 &\Rightarrow y_i^* = \frac{r_i(K_i - x_i^*)(1 + x_i^*)}{a_i K_i} \\ \frac{dy_j}{dt} = 0 &\Rightarrow x_i^* = \frac{-\rho_j s y_i^* + \rho_j s y_j^* + d_j y_j^*}{a_i \rho_j s y_i^* y_j^* - a_i \rho_j y_i^* y_j^* + \rho_j s y_i^* - \rho_j s y_j^* - d_j y_j^*} \end{aligned} \quad (4)$$

An equation of y_j^* is obtained by solving the following equation from Model (3):

$$\frac{dy_i}{dt} \rho_j + \frac{dy_j}{dt} \rho_i = \frac{a_i x_i y_i}{1 + x_i} \rho_j - d_i y_i \rho_j - d_j y_j \rho_i = 0 \Rightarrow y_j^* = \frac{\rho_j y_i^* (-a_i x_i^* + d_i x_i^* + d_i)}{d_j \rho_i (x_i^* + i)} \quad (5)$$

A substitution of y_i^* from (4) into y_j^* gives $y_j^* = \frac{r_i(K_i - x_i^*)[x_i^*(a_i - d_i) - d_i]\rho_j}{a_i K_i d_j \rho_i}$. The discussion above implies that the existence of the interior equilibrium requires $a_i > d_i$ and $\mu_i = \frac{d_i}{a_i - d_i} < x_i^* < K_i$ otherwise $y_j^* < 0$ or $y_i^* < 0$. Define

$$\begin{aligned} f_{t_i}(x_i) &= K_i(1 + x_i)[(a_i - d_i)(d_j + s\rho_j) - d_j s\rho_i] - K_i a_i(d_j + s\rho_j) \\ f_{b_i}(x_i) &= [d_i - (a_i - d_i)x_i][K_i(d_j + s\rho_j) + r_i \rho_j(1 - s)(1 + x_i)(1 + K_i)] + d_j K_i s(1 + x_i)\rho_i. \end{aligned}$$

Then we can conclude that x_i^* solving from Equation (4) is in term of y_i^* and y_j^* . Upon substitution of y_i^* and y_j^* into x_i^* we obtain the following nullclines:

$$\begin{aligned} x_i &= \frac{K_i(1 + x_i)[(a_i - d_i)(d_j + s\rho_j) - d_j s\rho_i] - K_i a_i(d_j + s\rho_j)}{[d_i - (a_i - d_i)x_i][K_i(d_j + s\rho_j) + r_i \rho_j(1 - s)(1 + x_i)(1 + K_i)] + d_j K_i s(1 + x_i)\rho_i} = \frac{f_{t_i}(x_i)}{f_{b_i}(x_i)} \\ &\Leftrightarrow \\ x_i f_{b_i}(x_i) - f_{t_i}(x_i) &= \underbrace{[x_i^3 - (\mu_i + K_i)x_i^2 - \alpha_i x_i + \beta_i]}_{f_i(x_i)} [x_i + 1] = 0 \end{aligned} \quad (6)$$

with $\beta_i = \frac{[d_j \rho_i s + d_i(d_j + \rho_j s)]K_i}{r_i(a_i - d_i)(1 - s)\rho_j}$ and

$$\alpha_i = \frac{[d_j s\rho_i + r_i d_i(1 - s) - (a_i - d_i)(d_j + s\rho_j)]K_i}{r_i(a_i - d_i)(1 - s)\rho_j} = \beta_i + \frac{[r_i d_i(1 - s) - a_i(d_j + s\rho_j)]K_i}{r_i(a_i - d_i)(1 - s)\rho_j}.$$

Based on the arguments above and additional analysis, we have the following proposition regarding the existence of the interior equilibria of Model (3):

Proposition 3.1. *Model (3) can have up to two interior equilibria $E_{x_i, y_i, y_j}^\ell = (x_{i\ell}^*, y_{i\ell}^*, y_{j\ell}^*)$, $\ell = 1, 2$. More specifically,*

1. *If $a_i < d_i$ or $K_i < \mu_i$ or $(\mu_i + K_i)^2 + 3\alpha_i < 0$, Model (3) has no interior equilibrium.*
2. *If $\frac{3\beta_i}{\mu_i + K_i} < \alpha_i < (\mu_i + K_i)^2$, then $f_i(x_i)$ has two positive roots $x_{i\ell}^*$, $\ell = 1, 2$. If, in addition, $\mu_i < x_{i\ell}^* < K_i$ for both $\ell = 1, 2$, then Model (3) has two interior equilibria.*

Notes: Proposition (3.1) implies that even if $f_i(x_i)$ has two positive real roots, Model (3) may have none or one interior equilibrium unless these two positive roots are in (μ_i, K_i) . Note that the interior equilibria of the subsystem Model (3) represent the boundary equilibria of Model (1) when $x_1 = 0 (i = 2)$ or $x_2 = 0 (i = 1)$. The existence of these boundary equilibria of Model (1) when $x_1 = 0$ or $x_2 = 0$ are hence guarantee by the conditions to obtain the interior equilibria E_{x_i, y_i, y_j}^ℓ and E_{y_j, x_i, y_i}^ℓ from Proposition (3.1).

In order to capture the dynamics of the interior equilibria of Model 3, we perform bifurcation simulations with respect to the proportion of predators using the passive dispersal, i.e., the values of s . Our analysis implies that Model (3) can have up to two interior equilibria $E_{x_1, y_1, y_2}^\ell = (x_{1\ell}^*, y_{1\ell}^*, y_{2\ell}^*)$ (for $i = 1$) and $E_{y_1, x_2, y_2}^\ell = (\hat{y}_{1\ell}^*, \hat{x}_{2\ell}^*, \hat{y}_{2\ell}^*)$ $\ell = 1, 2$ (for $i = 2$). We fix the following parameter values,

$$r_1 = 1, r_2 = 1.8, d_2 = 0.35, K_1 = 10, K_2 = 7, a_2 = 1.4, \rho_1 = 1, \rho_2 = 2.5.$$

These fixed values implies that at Patch 2, prey and predator coexist in the form of a unique stable limit cycle in the absence of dispersal since $\mu_2 = \frac{d_2}{a_2 - d_2} = 35/105 < (K_2 - 1)/2 = 3$. We consider the following two typical cases regarding the population dynamics of prey and predator in the absence of dispersal:

1. $d_1 = 0.85, a_1 = 1$: Predator and prey are persistent and have global equilibrium dynamics at Patch 1 in the absence of dispersal since $(K_1 - 1)/2 = 4.5 < \mu_1 = \frac{d_1}{a_1 - d_1} = 17/3 < 10 = K_1$.
2. $d_1 = 2, a_1 = 2.1$: Predator goes extinct globally at Patch 1 in the absence of dispersal since $\mu_1 = \frac{d_1}{a_1 - d_1} = 20 > K_1 = 10$.

The fixed values of parameters and the two cases above provide the following four scenarios:

1. $i = 1$ (i.e., $x_2 = 0$ for Model (1)) with $d_1 = 0.85, a_1 = 1$. In this case, Patch 1 is the source patch and Model (3) can have up to two interior equilibria depending on the values of s (see Figure 1(a)).
2. $i = 1$ (i.e., $x_2 = 0$ for Model (1)) with $d_1 = 2, a_1 = 2.1$. In this case, Patch 1 is the source patch and Model (3) has no interior equilibria according to Proposition (3.1).
3. $i = 2$ (i.e., $x_1 = 0$ for Model (1)) with $d_1 = 0.85, a_1 = 1$. In this case, Patch 2 is the source patch and Model (3) can have up to two interior equilibria depending on the values of s (see Figure 1(b)). The relative large value of s can stabilize the dynamics (see the blue region of Figure 1(b)).
4. $i = 2$ (i.e., $x_1 = 0$ for Model (1)) with $d_1 = 2, a_1 = 2.1$. In this case, Patch 2 is the source patch and Model (3) can have up to two interior equilibria depending on the values of s (see Figure 1(c)). The relative large value of s can stabilize the dynamics (see the blue region of Figure 1(c)).

The bifurcation diagrams (Figure 1) suggest that the proportion of predators using the passive dispersal can have huge impacts on the number of interior equilibria of Model (3): For the small

values of s , Model (3) can have one interior equilibrium (E_{x_1, y_1, y_2}^1 or E_{y_1, x_2, y_2}^1); For the intermediate values of s , Model (3) can have two interiors $E_{x_1, y_1, y_2}^l, l = 1, 2$ ($i = 1$) or $E_{y_1, x_2, y_2}^l, l = 1, 2$ ($i = 2$); For the large values of s , it has no interior equilibria. A more detail description of the effects of s on the interior equilibria of Model (3) is provided in Table (1).

Scenarios	$a_1 = 1$ and $d_1 = 0.85$				$a_1 = 2.1$ and $d_1 = 2$		
	$E_{x_1 y_1 y_2}^1$	$E_{x_1 y_1 y_2}^2$	$E_{y_1 x_2 y_2}^1$	$E_{y_1 x_2 y_2}^2$	$E_{x_1 y_1 y_2}^{1,2}$	$E_{y_1 x_2 y_2}^1$	$E_{y_1 x_2 y_2}^2$
$s \leq 0.1$	LAS	✗	Saddle	✗	✗	Saddle	✗
$0.15 \leq s \leq 0.45$	LAS	Saddle	Saddle	✗	✗	Saddle	✗
$0.55 \leq s \leq 0.62$	✗	✗	Saddle	✗	✗	LAS	Saddle
$0.68 < s < 0.82$	✗	✗	LAS	Saddle	✗	✗	✗
$s \geq 0.82$	✗	✗	✗	✗	✗	✗	✗

Table 1: Summary of the effect of the proportion of predators using the passive dispersal on Model (3) From Figures 1(a), 1(b), and 1(c). LAS refers to local asymptotical stability and ✗ implies the equilibrium does not exist.

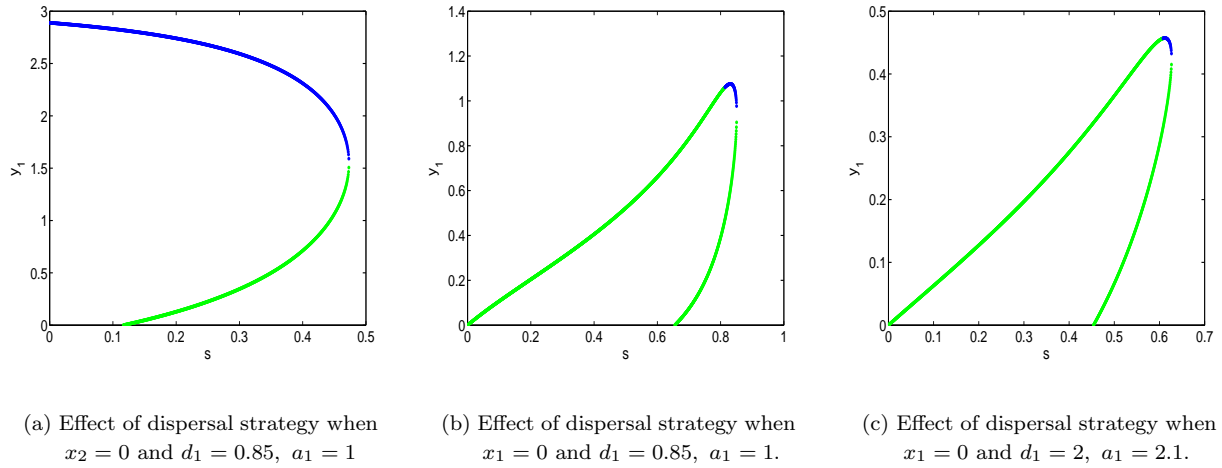


Figure 1: One parameter bifurcation diagrams of Model (3) with y -axis representing the population size of predator at Patch 1 and x -axis represent the proportion of predator using the passive dispersal. Figure 1(a) describes the number of interior equilibria ($\hat{x}_1^*, \hat{y}_1^*, \hat{y}_2^*$) when $x_2 = 0$ in Model (1) and their stability with respect to variation in s . Figure 1(b) and 1(c) describe the number of interior equilibria (y_1^*, x_2^*, y_2^*) of the submodel $x_2 = 0$ of Model (1) and their stability when s varies from 0 to 1. Blue represents the sink and green represents the saddle.

3.1. Boundary equilibria and global dynamics of Model (1)

First, we have boundary equilibria and global dynamics of Model (1) in the following theorem.

Theorem 3.2. [Boundary equilibria and global dynamics of Model (1)] Assume that $s \in (0, 1)$. Model (1) always has the following four boundary equilibrium

$$E_{0000}, E_{K_1 000}, E_{00 K_2 0}, E_{K_1 0 K_2 0}$$

with the first three always being saddle. $E_{K_1 0 K_2 0}$ is locally asymptotically stable if the following two inequalities in (7) hold:

$$\sum_{i=1}^2 \left[\frac{(a_i - d_i)(\mu_i - K_i)}{1 + K_i} + s\rho_i \right] > 0$$

and

$$\left[\frac{(a_1 - d_1)(\mu_1 - K_1)}{1 + K_1} \right] \left[s\rho_2 + \frac{(a_2 - d_2)(\mu_2 - K_2)}{1 + K_2} \right] + s\rho_1 \left[\frac{(a_2 - d_2)(\mu_2 - K_2)}{1 + K_2} \right] > 0. \quad (7)$$

And $E_{K_1 0 K_2 0}$ is saddle when one or both of equations (7) are not satisfied. In addition,

1. Model (1) is globally stable at $E_{K_1 0 K_2 0}$ if $\mu_i > K_i$ for both $i = 1, 2$.
2. At least prey population in one patch of Model (1) is persistent, and the predator population in each patch is persistent if $\mu_i < K_i$ for both $i = 1, 2$.

Notes: Theorem 3.2 indicates that the global stability of the boundary equilibrium $E_{K_1 0 K_2 0}$ does not depend on the proportion of predator population using the passive dispersal since $E_{K_1 0 K_2 0}$ is globally asymptotically stable when $\mu_i > K_i, i = 1, 2$ which is independent of s . However, the value of $s > 0$ and $\rho_i, i = 1, 2$ can stabilize $E_{K_1 0 K_2 0}$. For example, assume that $\mu_i < K_i$ and $\mu_j > K_j$, then in the absence of dispersal, the boundary equilibrium $E_{K_1 0 K_2 0}$ is a saddle. In the presence of the dispersal, according to Theorem 3.2, if we choose ρ_j large enough, then $E_{K_1 0 K_2 0}$ can be locally stable, thus the large dispersal at one patch may stabilize the boundary equilibrium $E_{K_1 0 K_2 0}$. However, if $s = 0$, then dispersal has no such effects.

Recall from Proposition (3.1) that the interior equilibria E_{x_1, y_1, y_2}^l and $E_{y_1, x_2, y_2}^l, l = 1, 2$ of Model (3) correspond to the boundary equilibria $E_{1\ell}^b = (x_{1\ell}^*, y_{1\ell}^*, 0, y_{2\ell}^*)$ and $E_{2\ell}^b = (0, \hat{y}_{1\ell}^*, \hat{x}_{2\ell}^*, \hat{y}_{2\ell}^*), \ell = 1, 2$ of Model (1). Based on Proposition (3.1), we could conclude that Model (1) has four such boundary equilibria. Figures 2 provide such an numerical example for the existence of the four boundary equilibria $E_{1\ell}^b = (x_{1\ell}^*, y_{1\ell}^*, 0, y_{2\ell}^*)$ and $E_{2\ell}^b = (0, \hat{y}_{1\ell}^*, \hat{x}_{2\ell}^*, \hat{y}_{2\ell}^*)$ under the following parameters:

$$s = 0.65, \quad r_1 = 1, \quad r_2 = 0.54, \quad d_1 = 0.45, \quad d_2 = 0.105, \quad K_1 = 10, \quad K_2 = 8, \quad a_1 = 0.6, \quad a_2 = 0.35, \quad \rho_1 = 1.75, \quad \rho_2 = 1.2.$$

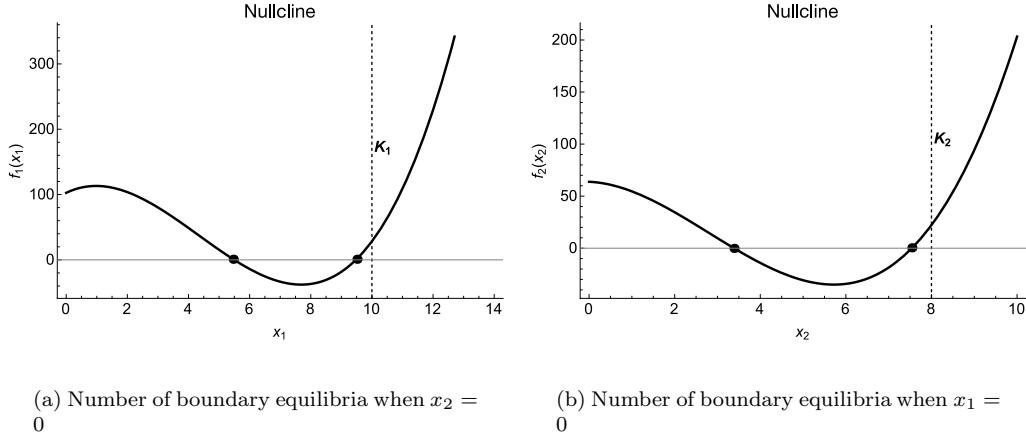


Figure 2: Boundary equilibria $E_{1\ell}^b = (x_{1\ell}^*, y_{1\ell}^*, 0, y_{2\ell}^*)$ and $E_{2\ell}^b = (0, \hat{y}_{1\ell}^*, \hat{x}_{2\ell}^*, \hat{y}_{2\ell}^*)$. Figure 2(a) and 2(b) are the cases when $s = 0.65$, $r_1 = 1$, $r_2 = 0.54$, $d_1 = 0.45$, $d_2 = 0.105$, $K_1 = 10$, $K_2 = 8$, $a_1 = 0.6$, $a_2 = 0.35$, $\rho_1 = 1.75$, and $\rho_2 = 1.2$. The solid lines are $f_1(x_1)$ and $f_2(x_2)$ while the dashed lines are K_1 and K_2 which illustrates the existence of boundary equilibria when $K_1 > x_{1\ell}^*$ or $K_2 > \hat{x}_{2\ell}^*$, $\ell = 1, 2$. The black dots represent real positive $x_{1\ell}^*$ and $\hat{x}_{2\ell}^*$ that satisfy existence of boundary equilibria, respectively.

We continue our study by analyzing the effects of s on the dynamics of the boundary equilibria $E_{1\ell}^b$ and $E_{2\ell}^b$, $\ell = 1, 2$ by adopting the same parameters in generating interior equilibria of Model (3) shown in Figure 1, i.e., let $d_1 = 0.85$, $a_1 = 1$ and $d_1 = 2$, $a_1 = 2.1$ and

$$r = 1.8, d_2 = 0.35, K_1 = 10, K_2 = 7, a_2 = 1.4, \rho_1 = 1, \rho_2 = 2.5.$$

Under these parameter values, we have the following two cases that are shown in Figure 3:

1. $d_1 = 0.85$, $a_1 = 1$: In this case, Model 1 can have up to three boundary equilibria depending on the values of s (see Figures 3(a), 3(b) and Table 2).
2. $d_1 = 2$, $a_1 = 2.1$: In this case, Model 1 can have up to two boundary equilibria depending on the values of s (see Figures 3(c) and Table 2).

We recapitulate the following dynamics regarding the effect of s on the equilibria $E_{1\ell}^b$ and $E_{2\ell}^b$, $\ell = 1, 2$: (1) Model (1) can have up to four boundary equilibria; (2) These boundary equilibria when exist are locally asymptotically stable or saddle; (3) Large s has a potential to destroy these equilibria. Also, observe the blue line for locally stable and green line for saddle in Figure 1(a) as oppose to only green line for saddle in Figure 3(a); this results suggest that the additional dimension from the three species Model (3) has a destabilization effect on the four species Model (1).

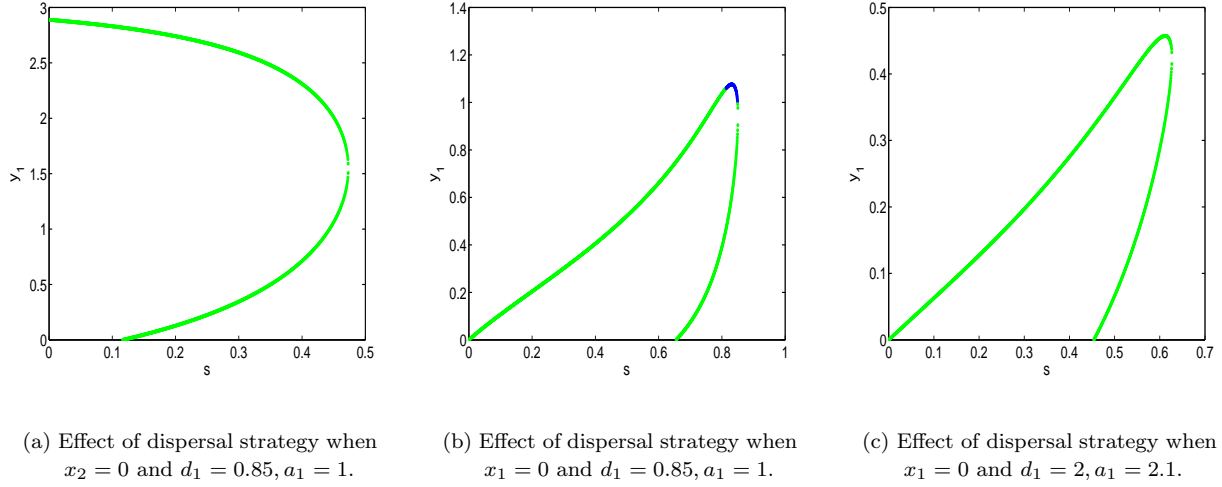


Figure 3: One parameter bifurcation diagrams of Model (1) with y -axis representing the population size of predator at Patch 1 and x -axis represent the proportion of predator using the passive dispersal. Figure 3(a) describes the number of boundary equilibria $E_{1\ell}^b = (x_{1\ell}^*, y_{1\ell}^*, 0, y_{2\ell}^*)$, $\ell = 1, 2$ from Model (1) and their stability with respect to variation in s when $d_1 = 0.85$, $a_1 = 1$. Figure 3(b) and 3(c) describes the number of boundary equilibria $E_{2\ell}^b = (0, \hat{y}_{1\ell}^*, \hat{x}_{2\ell}^*, \hat{y}_{2\ell}^*)$, $\ell = 1, 2$ from Model (1) and their change in stability when s varies from 0 to 1 with $d_1 = 0.85$, $a_1 = 1$ and $d_1 = 2$, $a_1 = 2.1$ respectively. Blue represents the sink and green represents the saddle.

Scenarios	$a_1 = 1$ and $d_1 = 0.85$				$a_1 = 2.1$ and $d_1 = 2$		
	E_{11}^b	E_{12}^b	E_{21}^b	E_{22}^b	$E_{11,12}^b$	E_{21}^b	E_{22}^b
$s \leq 0.1$	Saddle	✗	Saddle	✗	✗	Saddle	✗
$0.15 \leq s \leq 0.45$	Saddle	Saddle	Saddle	✗	✗	Saddle	✗
$0.55 \leq s \leq 0.62$	✗	✗	Saddle	✗	✗	Saddle	Saddle
$0.68 < s < 0.82$	✗	✗	LAS	Saddle	✗	✗	✗
$s \geq 0.82$	✗	✗	✗	✗	✗	✗	✗

Table 2: Summary of the effect of the proportion of predators using the passive dispersal on Model (3) From Figures 3(a), 3(b), and 3(c). LAS refers to local asymptotical stability and ✗ implies the equilibrium does not exist.

3.2. Interior equilibria and stability of Model (1)

Define $p_i(x) = \frac{a_i x}{1+x}$, $q_i(x) = \frac{r_i(K_i-x)(1+x)}{a_i K_i}$, and recall that $\mu_i = \frac{d_i}{a_i - d_i}$. Then from Model (1) we have the following equations

$$\begin{aligned} \frac{dx_i}{dt} &= r_i x_i \left(1 - \frac{x_i}{K_i}\right) - \frac{a_i x_i y_i}{(1+x_i)} = \frac{a_i x_i}{1+x_i} \left[\frac{r_i(K_i-x_i)(1+x_i)}{a_i K_i} - y_i \right] = p_i(x_i) [q_i(x_i) - y_i]. \\ \rho_j \frac{dy_i}{dt} + \rho_i \frac{dy_j}{dt} &= \rho_j y_i \left[\frac{a_i x_i}{1+x_i} - d_i \right] + \rho_i y_j \left[\frac{a_j x_j}{1+x_j} - d_j \right] = \rho_j y_i [p_i(x_i) - d_i] + \rho_i y_j [p_j(x_j) - d_j] \end{aligned}$$

Consider $(x_1^*, y_1^*, x_2^*, y_2^*)$ as an interior equilibrium of Model (1), then the following conditions must be satisfied:

$$q_i(x_i) - y_i = 0 \Leftrightarrow y_i = q_i(x_i)$$

and

$$\rho_j y_i [p_i(x_i) - d_i] + \rho_i y_j [p_j(x_j) - d_j] = 0 \Leftrightarrow \rho_j y_i [p_i(x_i) - d_i] = -\rho_i y_j [p_j(x_j) - d_j]$$

which yields the following by substituting the expression of $p_i(x)$ and $q_i(x)$ into (8)

$$x_i^2 - (\mu_i + K_i)x_i + \underbrace{\mu_i K_i + \frac{a_i K_i}{a_j K_j} \frac{\rho_i r_j}{\rho_j r_i} \frac{(a_j - d_j)}{(a_i - d_i)} (x_j - \mu_j)(x_j - K_j)}_{\phi_i(x_j)} = 0 \quad (9)$$

The equation (9) gives the following nullclines:

$$x_i = \frac{(\mu_i + K_i) \pm \sqrt{(\mu_i + K_i)^2 - 4\phi_i(x_j)}}{2} = F_i(x_j), \quad i, j = 1, 2, \quad i \neq j. \quad (10)$$

The complex form of (10) prevents us to obtain the explicit solutions of the interior equilibria of Model (1). We are going to explore the symmetric interior equilibrium for the symmetric Model (1) where we say that Model (1) is symmetric if $a_1 = a_2 = a$, $d_1 = d_2 = d$, $K_1 = K_2 = K$, $r_1 = r_2 = r$. Now we have the following theorem:

Theorem 3.3. *[The symmetric interior equilibrium and the stability] Suppose that Model (1) is symmetric with $r = 1$. We denote*

$$\mu = \frac{d}{a - d}, \quad \text{and} \quad \nu = \frac{(K - \mu)(1 + \mu)}{aK}.$$

Then $E = (\mu, \nu, \mu, \nu)$ is an unique symmetric interior equilibrium for Model (1). Moreover, E is locally asymptotically stable if $\frac{K-1}{2} < \mu < K$ while it is unstable if $\mu < \frac{K-1}{2}$ for $s \in [0, 1]$.

Notes: Theorem (3.3) implies the symmetric Model (1) has an unique symmetric interior equilibrium of the form $E = (\mu, \nu, \mu, \nu)$. The related results imply that dispersal of predators and s has no effect on the local stability of this symmetric interior equilibria when it exist since $\frac{K-1}{2} < \mu < K$ does not depend on $\rho_i, i = 1, 2$ or s . We note that Model (1) can have two additional interior equilibria in the symmetric case which can be locally stable or saddle depending on the value of s (see green line for saddle and blue line for locally stable in Figures 4(a) which correspond to the additional two boundary equilibria of Model (1) in the symmetric case). We consider the following fixed symmetric parameters:

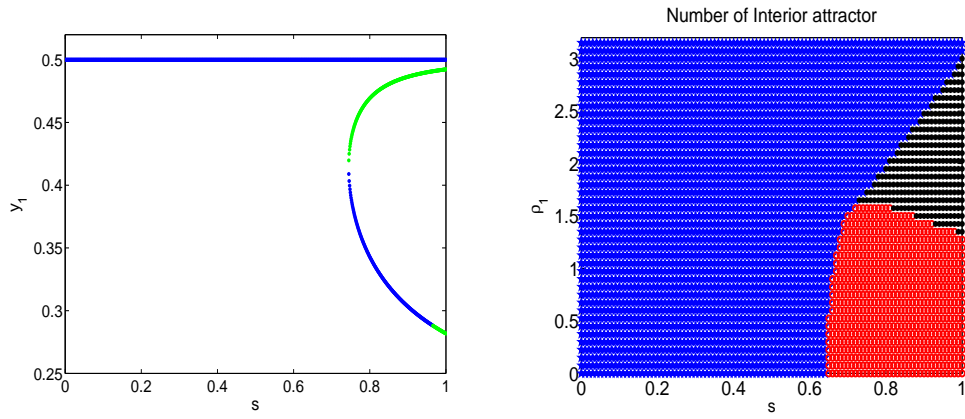
$$r_1 = r_2 = r = 1, \quad d_1 = d_2 = d = 5, \quad K_1 = K_2 = K = 10, \quad a_1 = a_2 = a = 6.$$

According to the bifurcation diagrams in Figures 4(a) and 4(b), Model (1) can have up to three interior equilibria in the symmetric case. It seems that the larger value of s can create two additional asymmetric interior equilibria which can be saddle or locally stable, thus generate bistability between two different interior attractors (See blue lines in Figure 4(a) when $0.78 \leq s \leq 0.92$). The local stability of $E = (\mu, \nu, \mu, \nu)$ does not depend on s as illustrated in Theorem 3.3.

Summary: In addition to the summary of our analysis listed in Table (3), we summarize the following dynamics of Model (1) base on mathematical analysis and bifurcation diagrams from our study:

1. The four basic boundary equilibria E_{0000} , E_{K_1000} , E_{00K_20} , $E_{K_10K_20}$ always exist where E_{0000} , E_{K_1000} , E_{00K_20} , are always saddle while $E_{K_10K_20}$ is locally asymptotically stable if the two inequalities 7 are satisfied. Large dispersal of predators can stabilize the boundary equilibrium $E_{K_10K_20}$ when $s \in (0, 1]$. However, the value of s has no effects on the global stability of the boundary equilibrium $E_{K_10K_20}$.
2. Model (1) can have up to four other boundary equilibria $E_{1\ell}^b = (x_{1\ell}^*, y_{1\ell}^*, 0, y_{2\ell}^*)$ and $E_{2\ell}^b = (0, \hat{y}_{1\ell}^*, \hat{x}_{2\ell}^*, \hat{y}_{2\ell}^*)$ for $\ell = 1, 2$. The number of these boundary equilibria and the stability could be affected by the dispersal strength $\rho_i, i = 1, 2$ and the values of s . For example, the large values of s can destroy these boundary equilibria.
3. In the symmetric case, Model (1) may potentially have three interior equilibria including $E = (\mu, \nu, \mu, \nu)$ from Theorem 3.3 when $a > d$. Although the local stability of E does not depend on s , the large value of s can generate the two additional asymmetric interior equilibria, hence, create multiple interior attractors.

Define $\mu_i = \frac{d_i}{a_i - d_i}$, $\nu_1 = \frac{(K_1 - \mu_1)(1 + \mu_1)}{a_1 K_1}$, $\nu_2 = \frac{r(K_2 - \mu_2)(1 + \mu_2)}{a_2 K_2}$, $\hat{\mu}_i = \frac{\hat{d}_i}{a_i - \hat{d}_i}$, $\hat{\nu}_i = q_i(\hat{\mu}_i) = \frac{r_i(K_i - \hat{\mu}_i)(1 + \hat{\mu}_i)}{a_i K_i}$, $\hat{\nu}_j^i = \frac{\rho_j \hat{\nu}_i}{d_j + \rho_j}$ where $\hat{d}_i = d_i + \frac{\rho_i d_j}{d_j + \rho_j}$ $i, j = 1, 2, i \neq j$ and $E_{12}^{b*} = E_{\mu_1 \nu_1 K_2 0}$, $E_{22}^{b*} = E_{K_1 0 \mu_2 \nu_2}$. Then the boundary dynamics for $s = 0, 1$ from the work of (Jansen, 2001; Kang et al., 2014) and $s \in (0, 1)$ from our current work is summarize in Table 3.



(a) s V.S. y_1 for the effect of s when Model (1) is symmetric with $\rho_1 = 1.72$ and $\rho_2 = 13$

(b) s V.S. ρ_1 for the number of interior equilibria when Model (1) is symmetric and $\rho_2 = 13$

Figure 4: One and two parameter bifurcation diagrams of symmetric Model (1) with y -axis representing the population size of predator at Patch 1 in figure 4(a). We used the following parameters $r = 1$, $d = 5$, $K = 10$, and $a = 6$. Figure 4(a) describes the number of interior equilibria and their change in stability when s varies from 0 to 1. Blue line represents sink and green line represents saddle in Figure 4(a). Figure 4(b) describes how the number of interior equilibria change for different values of dispersal strategy s and dispersal rate ρ_1 . Black region have three interior equilibria; red regions have two interior equilibria; and blue regions have one interior equilibrium in Figure 4(b).

Scenarios	Existence condition, Local and Global stability of Model (1)		
	$s = 0$	$s \in (0, 1)$	$s = 1$
$E_{0000}, E_{K_1 000}, E_{00 K_2 0}$	Always exist and always saddle	Always exist and always saddle	Always exist and always saddle
$E_{K_1 0 K_2 0}$	Always exist; LAS and GAS if $\mu_i > K_i$ for both $i = 1, 2$	Always exist; GAS if $\mu_i > K_i$ for both $i = 1, 2$; while LAS if Equations 7 are satisfied	Always exist; GAS if $\mu_i > K_i$ for both $i = 1, 2$; LAS if condition (1) is satisfied
$E_{1\ell}^b (x_i = 0), \ell = 1, 2, i = 1, 2$	Do not exist	One or two exist if $\frac{3\beta_j}{\mu_j + K_j} < \alpha_j < (\mu_j + K_j)^2$ with $i, j = 1, 2, i \neq j$; Can be locally asymptotically stable or saddle as shown in Figures 3(a), 3(b), 3(c)	Exist if $0 < \hat{\mu}_i < K_i$; LAS if $\frac{K_i - 1}{2} < \hat{\mu}_i < K_i$ and $r_j < a_j \hat{\nu}_j^i$. GAS if $\frac{K_i - 1}{2} < \hat{\mu}_i < K_i$ and $\frac{r_j (K_j + 1)^2}{4a_j K_j} < \hat{\nu}_i^j, i, j = 1, 2, i \neq j$.
$E_{i2}^{b*}, i, j = 1, 2, i \neq j$	Exist if $0 < \mu_i < K_i$; LAS if $\frac{K_i - 1}{2} < \mu_i < K_i$ and condition (2) is satisfied	Do not exist	Do not exist
Condition 1: Condition 2:	$\sum_{i=1}^2 \left[\frac{(a_i - d_i)(\mu_i - K_i)}{1 + K_i} + \rho_i \right] > 0 \text{ and } \left[\frac{(a_1 - d_1)(\mu_1 - K_1)}{1 + K_1} \right] \left[\rho_2 + \frac{(a_2 - d_2)(\mu_2 - K_2)}{1 + K_2} \right] + \rho_1 \left[\frac{(a_2 - d_2)(\mu_2 - K_2)}{1 + K_2} \right] > 0$ $0 < \frac{d_i}{a_j - d_i} < K_j < \mu_j \text{ and } \rho_j < \frac{d_j - K_j(a_j - d_j)}{\nu_i [K_j(a_j - d_i) - d_i]}; i, j = 1, 2, i \neq j$		

Table 3: Summary of the local and global dynamic of Model (1). LAS refers to the local asymptotical stability, and GAS refers to the global stability.

4. Effects of dispersal strategies on the prey-predator population dynamics

In order to get more insights into the dynamics of Model (1), we perform bifurcation analysis in this section. We fixed the following parameters for most of the simulations

$$r = 1.8, d_2 = 0.35, K_1 = 10, K_2 = 7, a_2 = 1.4, \rho_1 = 1, \rho_2 = 2.5.$$

and consider these two cases: $d_1 = 0.85, a_1 = 1$ and $d_1 = 2, a_1 = 2.1$. According to the dynamics of the subsystem Model (2) provided in Section 2, we know that in the absence of dispersal, Patch 1 has global stability at $(10, 0)$ if $\frac{d_1}{a_1 - d_1} > 10$ (e.g., when $d_1 = 2, a_1 = 2.1$) and it has global stability at its unique interior $\left(\frac{d_1}{a_1 - d_1}, \frac{(10 - \frac{d_1}{a_1 - d_1})(1 + \frac{d_1}{a_1 - d_1})}{10a_1} \right)$ if $4.5 < \frac{d_1}{a_1 - d_1} < 10$ (e.g., when $d_1 = 0.85, a_1 = 1$); while Patch 2 has a unique stable limit cycle since $d_2 = 0.35, K_2 = 7, a_2 = 1.4$.

We implement one and two parameters bifurcation diagrams to obtain insights into the dynamical patterns of the asymmetric two patch Model (1) in the following way:

1. $d_1 = 0.85$ and $a_1 = 1$: In the absence of dispersal, the uncoupled two patch model is unstable at the interior equilibrium $(5.67, 288.89, 0.33, 80)$. However, in the presence of the dispersal, Figure 5(a) (blue regions) suggest that the intermediate values of s can stabilize the dynamics

while the large values of s with certain dispersal strengths could generate multiple interior equilibria (up to three interior equilibria), thus lead to multiple attractors potentially. Moreover, two dimensional bifurcation diagram shown in Figure 5(b) suggest that the large values of s combined with the small or large dispersal strength ρ_1 in Patch 1 can destroy the interior equilibria (see white regions in Figure 5(b)) with consequences that prey in one patch may go extinct but predator persists in each patch. Table (4) provides a more details description on the existence and stability of the interior equilibria of Model (1).

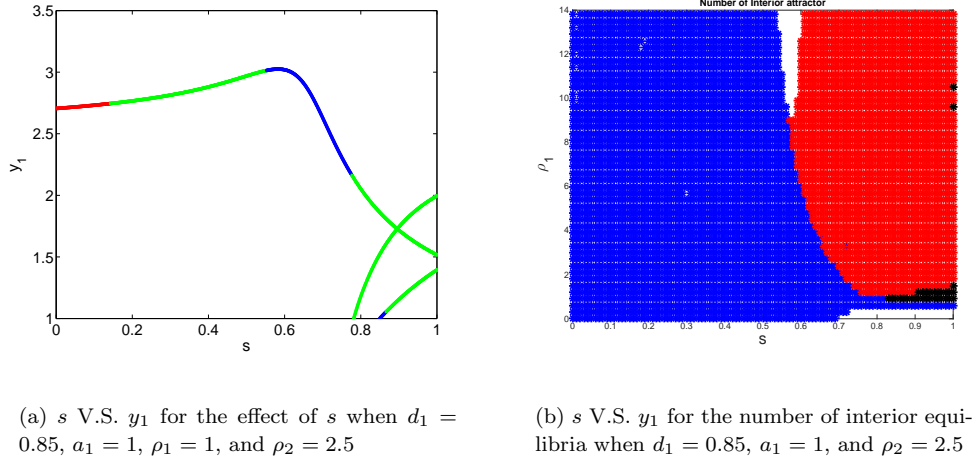


Figure 5: One and two parameter bifurcation diagrams of Model (1) with y -axis representing the population size of predator at Patch 1 in Figure 5(a). The following parameters are used: $r = 1.8$, $d_2 = 0.35$, $K_1 = 10$, $K_2 = 7$, and $a_2 = 1.4$. Figure 5(a) describes the number of interior equilibria and their change in stability when s varies from 0 to 1. Blue line represents sink, green line represents saddle, and red line represents source in Figure 5(a). Figure 5(b) describes how the number of interior equilibria change for different values of s and dispersal rate ρ_1 . Black region have three interior equilibria; red regions have two interior equilibria; blue regions have one interior equilibrium, and white regions have no interior equilibria in Figure 5(b).

Scenarios	$a_1 = 1$ and $d_1 = 0.85$			$a_1 = 2.1$ and $d_1 = 2$		
	$E^1_{x_1 y_1 x_2 y_2}$	$E^2_{x_1 y_1 x_2 y_2}$	$E^3_{x_1 y_1 x_2 y_2}$	$E^1_{x_1 y_1 x_2 y_2}$	$E^2_{x_1 y_1 x_2 y_2}$	$E^3_{x_1 y_1 x_2 y_2}$
$s \leq 0.07$	Source	\times	\times	Saddle	Source	LAS
$0.9 \leq s \leq 0.15$	Source	\times	\times	Saddle	Saddle	LAS
$0.2 \leq s \leq 0.43$	Saddle	\times	\times	LAS	Saddle	Saddle
$0.55 \leq s \leq 0.68$	LAS	\times	\times	LAS	\times	\times
$0.78 \leq s \leq 0.82$	Saddle	Saddle	\times	Saddle	\times	\times
$0.83 \leq s \leq 0.84$	Saddle	Saddle	LAS	Saddle	\times	\times
$s \geq 0.84$	Saddle	Saddle	Saddle	Saddle	\times	\times

Table 4: Summary of the effect of the proportion of predators using the passive dispersal on the interior equilibria of Model (1) From Figures 5(a), and 6(a). LAS refers to local asymptotical stability, \times implies the equilibrium does not exist, and $E^i_{x_1 y_1 x_2 y_2}$, $i = 1, 2, 3$ are the three possible interior equilibria of Model (1).

2. $d_1 = 2$ and $a_1 = 2.1$: In the absence of dispersal, the uncoupled two patch model has extinction

of predator in Patch 1 and is unstable at the boundary equilibrium $(10, 0, 0.33, 80)$. However, in the presence of the dispersal, Figure 6(a) (blue regions) suggest that the intermediate values of s can stabilize the dynamics while the small values of s with certain dispersal strengths could generate multiple interior equilibria (up to three interior equilibria), thus lead to multiple attractors potentially. Moreover, two dimensional bifurcation diagram shown in Figure 6(b) suggest that the large values of s combined with the large dispersal strength ρ_1 in Patch 1 can destroy the interior equilibria (see white regions in Figure 5(b)) with consequences that prey in one patch may go extinct but predator persists in each patch. A more detail dynamic from Figure 6(b) is presented in Table (4).

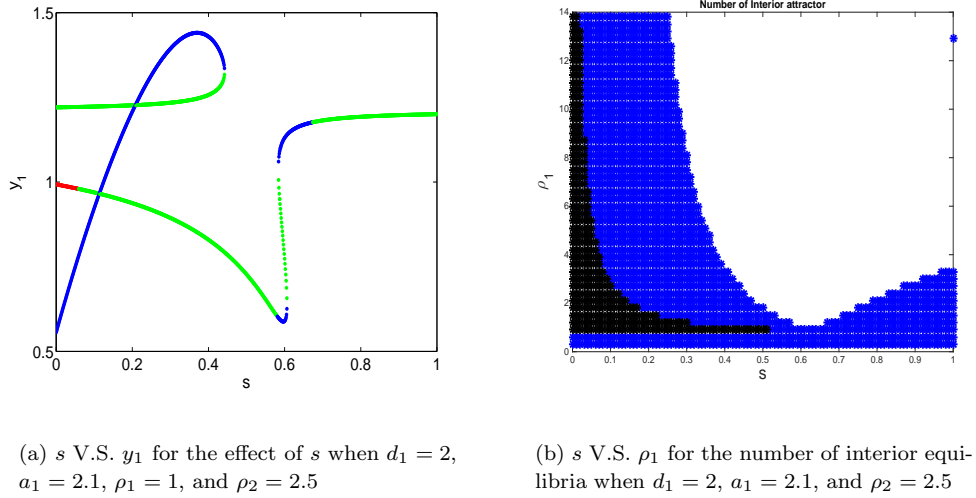
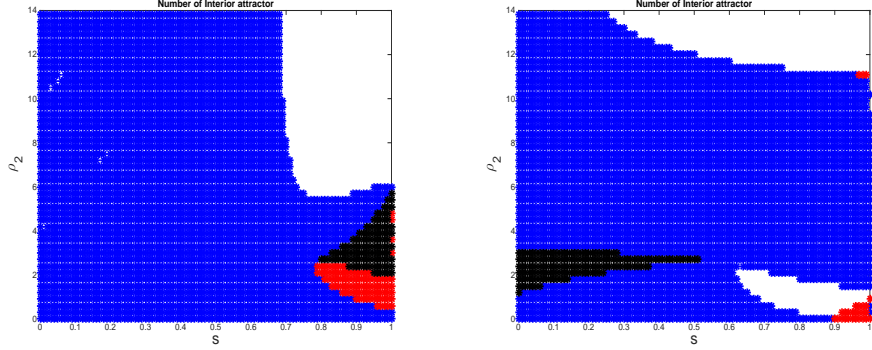


Figure 6: One and two parameter bifurcation diagrams of Model (1) with y -axis representing the population size of predator at Patch 1 in figure 6(a). We used the following parameters $r = 1.8$, $d_2 = 0.35$, $K_1 = 10$, $K_2 = 7$, and $a_2 = 1.4$. Figure 6(a) describes the number of interior equilibria and their change in stability when s varies from 0 to 1 under the parameters $d_1 = 2$ and $a_1 = 2.1$. Blue represents sink, green represents saddle, and red represents source. Figure 6(b) describes how the number of interior equilibria change for different values of dispersal strategy s and dispersal rate ρ_1 . Black region have three interior equilibria; red regions have two interior equilibria; blue regions have one interior equilibrium, and white regions have no interior equilibria.

- Two parameter bifurcation diagrams of the relative dispersal rate ρ_2 versus the dispersal strategy s for both scenarios of $d_1 = 0.85$, $a_1 = 1$ (Figure 7(a)) and $d_1 = 2$, $a_1 = 2.1$ (Figure 7(b)). For both cases, the large s combined with the large dispersal strength in Patch 2, i.e., ρ_2 , can destroy the interior equilibrium (see white regions in Figures 7(a) and 7(b) for $s > 0.6$); while the small s (for $d_1 = 0.85$, $a_1 = 1$) and the large value of s (for $d_1 = 2$, $a_1 = 2.1$) could generate multiple interior equilibria (see black region for three interior equilibria and red region for two interior equilibria in Figure 7(a) and 7(b)).



(a) s V.S. ρ_2 for the number of interior equilibria when $d_1 = 0.85$ and $a_1 = 1$

(b) s V.S. ρ_2 for the number of interior equilibria when $d_1 = 2$ and $a_1 = 2.1$

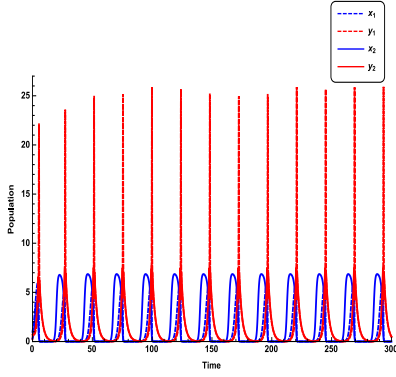
Figure 7: Two parameters bifurcation diagrams of Model (1) with y -axis representing the relative dispersal rate ρ_2 and x -axis represent the strength of dispersal mode s . The following parameters are used: $r = 1.8$, $d_2 = 0.35$, $K_1 = 10$, $K_2 = 7$, $a_2 = 1.4$, and $\rho_1 = 1$. Both figures 7(a) and 7(b) describes how the number of interior equilibria change for different values of dispersal strategy s and dispersal rate ρ_2 where the parameters $d_1 = 0.85$, $a_1 = 1$ are used for the left figure 7(a) while $d_1 = 2$, $a_1 = 2.1$ are used for the right figure 7(b) in addition to the fixed parameters. Black region have three interior equilibria; red regions have two interior equilibria; blue regions have one interior equilibrium, and white regions have no interior equilibria in Figures 7(a) and 7(b).

No interior equilibrium but all species coexist with fluctuating dynamics: Our discussions above suggest that the large values of s can destroy the interior equilibrium (see white regions in Figures 5(b), 6(b), 7(a) and 7(b)). Thus, the system is not permanent based on the fixed point theorem. However, our time series (e.g., Figures 8(a) and 8(b)) suggest that for almost all strictly positive initial conditions, both prey and predator can coexist through fluctuating dynamics for some white regions of Figures 7(a) and 7(b).

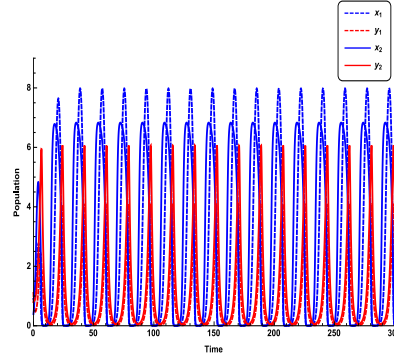
The proportion of the predators population engaging in the passive dispersal, i.e., s , has profound impacts on the population dynamics of prey and predator presented by Model (1) which generate complicated dynamics including different types of multiple attractors.

Boundary attractor versus an interior attractor through two interior equilibria: When Model (1) has two interior equilibria, the typical dynamics are that Model (1) either converges to a boundary attractor or the interior attractor depending initial conditions. We provide an example in Figures 9(a), and 9(b) where $a_1 = 1$, $d_1 = 0.85$, $s = 0.8$ and

$$r = 1.8, d_2 = 0.35, K_1 = 10, K_2 = 7, a_2 = 1.4, \rho_1 = 1, \rho_2 = 2.5.$$

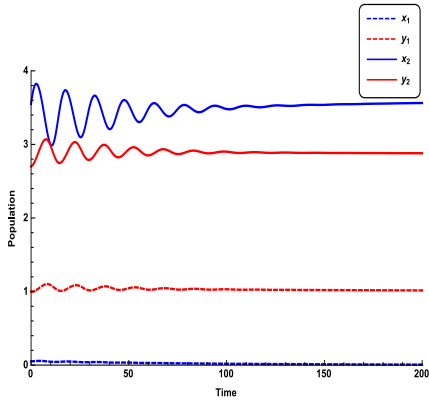


(a) Time series of Model 1 when $a_1 = 1$, $d_1 = 0.85$, $s = 0.55$, $\rho_1 = 13$, $x_1(0) = 1$, $y_1(0) = 0.25$, $x_2(0) = 0.3$, and $y_2(0) = 0.7$.

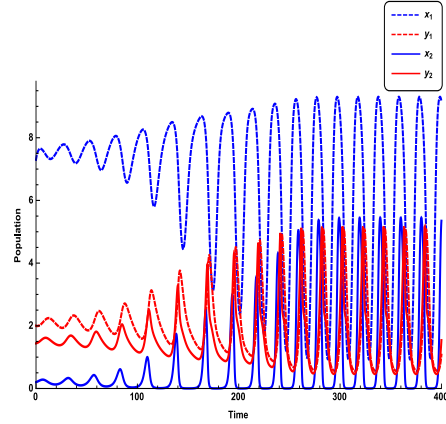


(b) Time series of Model 1 when $a_1 = 2.1$, $d_1 = 2$, $\rho_1 = 1$, $\rho_2 = 0.75$, $s = 0.85$, $x_1(0) = 0.9$, $y_1(0) = 1.1$, $x_2(0) = 0.4$, and $y_2(0) = 0.8$.

Figure 8: Time series of Model 1 when $r = 1.8$, $d_2 = 0.35$, $K_1 = 10$, $K_2 = 7$, and $a_2 = 1.4$. Figures 8(a) and 8(b) illustrate the coexistence of prey and predator through fluctuating dynamics while Model 1 has no interior equilibria. The blue dashed lines represent the prey population in patch 1, the dashed red lines represent the predator population in patch 1, the blue solid lines is the the prey population in patch 2, and the red solid lines represent predator population in patch 2.



(a) Time series of Model 1 when $a_1 = 1$, $d_1 = 0.85$, $s = 0.8$, $x_1(0) = 0.05$, $y_1(0) = 1$, $x_2(0) = 3.55$, and $y_2(0) = 2.7$ which converges to the boundary equilibrium $(x_1, y_1, x_2, y_2) = (0, 1, 3.6, 2.9)$.



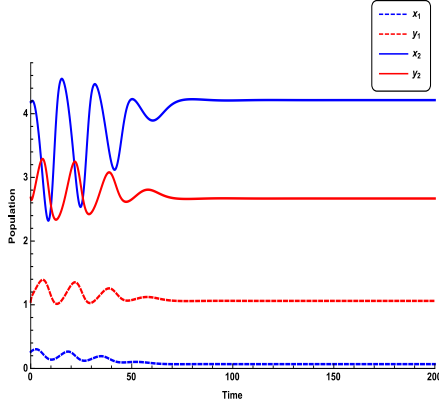
(b) Time series of Model 1 when $a_1 = 1$, $d_1 = 0.85$, $s = 0.8$, $x_1(0) = 0.2$, $y_1(0) = 1.15$, $x_2(0) = 2.7$, and $y_2(0) = 2.8$.

Figure 9: Time series of Model 1 when $r = 1.8$, $d_2 = 0.35$, $K_1 = 10$, $K_2 = 7$, $a_2 = 1.4$, $\rho_1 = 1$, and $\rho_2 = 2.5$. Figures 9(a) and 9(b) represent the dynamical pattern generated by two interior saddles, one boundary sink and one boundary saddle. The blue dashed lines represent the prey population in patch 1, the dashed red lines represent the predator population in patch 1, the blue solid lines is the the prey population in patch 2, and the red solid lines represent predator population in patch 2.

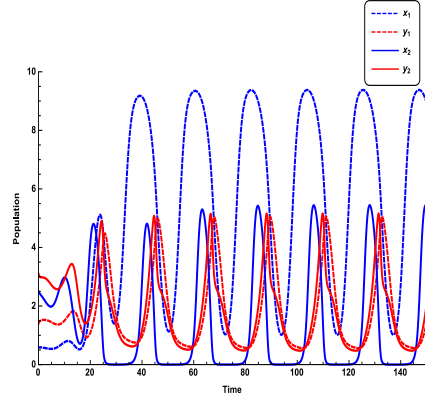
Two interior attractors through three interior equilibria: When Model (1) has three interior

equilibria, the typical dynamics are that Model (1) has two interior attractors. We provide an example in Figures 10(a), and 10(b) where $a_1 = 1$, $d_1 = 0.85$, $s = 0.8392$ and

$$r = 1.8, d_2 = 0.35, K_1 = 10, K_2 = 7, a_2 = 1.4, \rho_1 = 1, \rho_2 = 2.5.$$



(a) Time series of Model 1 when $a_1 = 1$, $d_1 = 0.85$, $s = 0.8392$, $x_1(0) = 0.25$, $y_1(0) = 1.05$, $x_2(0) = 4.18$, and $y_2(0) = 2.68$ which stabilize at $(x_1, y_1, x_2, y_2) = (0.09, 1.08, 4.27, 2.64)$.



(b) Time series of Model 1 when $a_1 = 1$, $d_1 = 0.85$, $s = 0.8392$, $x_1(0) = 0.58$, $y_1(0) = 1.4$, $x_2(0) = 2.5$, and $y_2(0) = 3.1$.

Figure 10: Time series of Model 1 when $r = 1.8$, $d_2 = 0.35$, $K_1 = 10$, $K_2 = 7$, $a_2 = 1.4$, $\rho_1 = 1$, and $\rho_2 = 2.5$. Figures 10(a) and 10(b) describe the dynamical pattern generated by two interior saddles and one interior that is locally stable. The blue dashed lines represent the prey population in patch 1, the dashed red lines represent the predator population in patch 1, the blue solid lines is the the prey population in patch 2, and the red solid lines represent predator population in patch 2.

5. Conclusion

We propose and study a two patch prey predator model with the following assumptions: (1) Only predators can migrate and preys are immobile; (2) predators use two dispersal strategies: the passive dispersal and the predation attraction; (3) The model is reduced to the Rosenzweig-MacArthur model in the absence of dispersal. We provide boundedness and positivity of the proposed model in Theorem 2.1. The analytical results which is summarize in Table (3) along with the numerical results presented throughout the paper answer the questions regarding the dynamics of our proposed nonlinear model:

When there is no prey in one of the patches, our model applies to the sink-source dynamics where no prey patch is the sink. Analytical results (Theorem 3.1) imply that predators could be driven to extinction locally if the product of the dispersal strength and the proportion of predator population using the passive dispersal (i.e. s) are large. In addition, the sink-source dynamics can process two interior equilibria (see Proposition (3.1)). Our simulations (Figure 1) suggest that

the small values of s lead to permanence of the system which is supported by Theorem 3.1. For the intermediate values of s , the system can have two interior equilibria $E_{x_1, y_1, y_2}^l, l = 1, 2$ ($i = 1$) or $E_{y_1, x_2, y_2}^l, l = 1, 2$ ($i = 2$); For the large values of s , it has no interior equilibria with the consequences that predator goes extinct in two patches. In addition, the intermediate values of s can stabilize the dynamics with certain dispersal strengths (see blue line for locally stable in Figures 1(a), 1(b), and 1(c)).

Theorem (3.2) and Proposition (3.1) provide the existence of the boundary equilibria and the related local stability of our model (1). These results illustrate how s can potentially stabilize the basic boundary equilibria $E_{K_1 0 K_2 0}$ consequently driving predator extinct in both patches locally. Theorem (3.3) provide insights into the existence and stability of a symmetric interior equilibria when Model (1) is symmetric (i.e. in exception of the dispersal strength and dispersal strategy, all life history parameters are the same in both patches). The analytical results indicate that the dispersal strategies do not affect the existence and stability of this symmetric interior equilibria denoted E . However, bifurcation diagrams shown in Figures 4(a) and 4(b) suggest that the large predator population using the passive dispersal could generate two additional asymmetric interior equilibria which can be saddle or locally stable, thus generate bistability between two different attractors (see blue lines in Figure 4(a) when $0.78 \leq s \leq 0.92$).

Our numerical simulations performed in Section 4 show that the dispersal strategies, i.e., the portion of predator population using the passive dispersal strategies, have huge impacts on the prey and predator populations in two patches. The intermediate predator population using the passive dispersal tends to stabilize the dynamics. Depending on the other life history parameters, the large or small predator population using the passive dispersal with certain dispersal strengths could generate multiple interior equilibria (up to three interior equilibria), thus lead to multiple attractors potentially. When Model (1) has two interior equilibria, it either converges to a boundary attractor or the interior attractor depending initial conditions (see Figures 9(a), and 9(b)); when Model (1) has three interior equilibria, it can have two interior equilibria (see Figures 10(a), and 10(b)). The large predator population using the passive dispersal combined with the large dispersal strength can destroy the interior equilibria with consequences that prey in one patch may go extinct but predator persists in each patch. However, there are situations when the two patch model has no interior equilibrium but all species coexist with fluctuating dynamics (see Figures 8(a) and 8(b)).

The summary of our finding illustrates how population dynamics of prey and predators are affected by changing their foraging behavior. This study give us a better understanding on how combinations of different foraging strategies used by predator favor or affect their coexistence or extinction. Many species tend to adapt to environmental conditions and change their foraging behavior accordingly (see example of foraging behavior of Ants in Markin (1970); Taylor (1977); Traniello et al. (1984)). It will be interesting to look at a two patch prey predator model with adaptive foraging behavior in which adaptation is driven by certain environmental conditions such as temperature or availability of local resources. Such work is on going by the authors.

6. Appendix: Proofs

Proof of Theorem 2.1

Proof. Observed that $\frac{dx_i}{dt}|_{x_i=0} = 0$ and $\frac{dy_i}{dt}|_{y_i=0} = \rho_i s y_j \geq 0$ if $y_j \geq 0$ for $i = 1, 2$, $j = 1, 2$, and $i \neq j$. The model (1) is positively invariant in \mathbb{R}_+^4 by theorem A.4 (p. 423) in Thieme (2003). It follows that the set $\{(x_1, y_1, x_2, y_2) \in \mathbb{R}_+^4 : x_i = 0\}$ is invariant for both $i = 1, 2$ under the same theorem. The proof of boundedness is as follow

$$\frac{dx_i}{dt} = r_i x_i \left(1 - \frac{x_i}{K_i}\right) - \frac{a_i x_i y_i}{1 + x_i} \leq r_i x_i \left(1 - \frac{x_i}{K_i}\right)$$

thus

$$\limsup_{t \rightarrow \infty} x_i(t) \leq K_i.$$

Now we define $L = \rho_2(x_1 + y_1) + \rho_1(x_2 + y_2)$, to get

$$\begin{aligned} \frac{dL}{dt} &= \rho_2 \frac{d(x_1 + y_1)}{dt} + \rho_1 \frac{d(x_2 + y_2)}{dt} \\ &= \rho_2 x_1 \left(1 - \frac{x_1}{K_1}\right) + \rho_1 r x_2 \left(1 - \frac{x_2}{K_2}\right) - \rho_2 d_1 y_1 - \rho_1 d_2 y_2 + \rho_1 \rho_2 (1 - s) \left(\frac{a_1 x_1 y_1 y_2}{1 + x_1} - \frac{a_2 x_2 y_2 y_1}{1 + x_2}\right) \\ &\quad - \rho_1 \rho_2 (1 - s) \left(\frac{a_1 x_1 y_1 y_2}{1 + x_1} - \frac{a_2 x_2 y_2 y_1}{1 + x_2}\right) + \rho_1 \rho_2 s (y_1 - y_2) - \rho_1 \rho_2 s (y_1 - y_2) \\ &= \rho_2 x_1 \left(1 - \frac{x_1}{K_1} + d_1\right) + \rho_1 x_2 \left(r - \frac{r x_2}{K_2} + d_2\right) - \rho_2 d_1 (x_1 + y_1) - \rho_1 d_2 (x_2 + y_2) \\ &\leq T - d_{\min} [\rho_2(x_1 + y_1) + \rho_1(x_2 + y_2)] = T - d_{\min} L \end{aligned}$$

where $d_{\min} = \min\{d_1, d_2\}$ and

$$T = \max_{0 \leq x_1 \leq K_1} \left\{ \rho_2 x_1 \left(1 - \frac{x_1}{K_1} + d_1\right) \right\} + \max_{0 \leq x_2 \leq K_2} \left\{ \rho_1 x_2 \left(r - \frac{r x_2}{K_2} + d_2\right) \right\}.$$

consequently

$$\limsup_{t \rightarrow \infty} L(t) = \limsup_{t \rightarrow \infty} \rho_2(x_1(t) + y_1(t)) + \rho_1(x_2(t) + y_2(t)) \leq \frac{T}{d_{\min}}.$$

This shows that Model (1) is bounded in \mathbb{R}_+^4 which conclude the proof of theorem (2.1). \square

Proof of Theorem 3.1

Proof. Item 1: Model (1) is positively invariant and bounded in \mathbb{R}_+^4 according to Theorem 2.1. From this, it follows that Model (1) is attracted to a compact set C in \mathbb{R}_+^4 . Furthermore, if $x_j = 0$, $j = 1$, or 2 , then Model (1) is reduced to three species couple models (3). Consider the fact that $\lim_{t \rightarrow \infty} y_i(t) = \lim_{t \rightarrow \infty} y_j(t) = 0$ when $x_i = 0$, we can conclude that $y_1 = y_2 = 0$ is an omega limit set of Model (3). Additionally

$$\frac{dx_i}{x_i dt} \Big|_{x_i=0} = r_i > 0$$

then by Theorem 2.5 of Hutson (1984) (Hutson, 1984), prey x_i persists.

Item 2: Define $V(y_i, y_j) = \rho_j y_i + \rho_i y_j$, then we have

$$\frac{dV}{dt} = \frac{a_i x_i y_i}{1 + x_i} \rho_j - d_i y_i \rho_j - d_j y_j \rho_i = \left[\frac{a_i x_i}{1 + x_i} - d_i \right] y_i \rho_j - d_j y_j \rho_i.$$

Notice that $\limsup_{t \rightarrow \infty} x_i(t) \leq K_i$. Then if $\mu_i > K_i$ we have $\frac{a_i K_i}{1 + K_i} - d_i < -\delta < 0$ and let $\delta^* = \min\{\delta, d_j\}$. This implies

$$\begin{aligned} \frac{dV}{dt} &= \left[\frac{a_i x_i}{1 + x_i} - d_i \right] y_i \rho_j - d_j y_j \rho_i < -(\delta y_i \rho_j + d_j y_j \rho_i) \\ &< -\delta^* (y_i \rho_j + d_j y_j \rho_i) = -\delta^* V(y_i, y_j) \end{aligned}$$

Therefore both predators go extinct if $\mu_i > K_i$. Now Model (3) reduces to the following prey model since $\limsup_{t \rightarrow \infty} y_i(t) = \limsup_{t \rightarrow \infty} y_j(t) = 0$

$$\frac{dx_i}{dt} = r_i x_i \left(1 - \frac{x_i}{K_i} \right)$$

with prey x_i converging to K_i . Thus Model (3) is globally stable at $(K_i, 0, 0)$ when $\mu_i > K_i$.

Item 3: Now we focus on the persistence condition for predator y_i . Since x_i is persistent from Item 1 Theorem 3.1 then we can conclude that Model (3) is attracted to a compact set C_s subset of C that exclude E_{000} . Then according to Theorem 2.1 and 3.2, the omega limit set of Model (3) on the compact set C_s is $E_{K_i, 00}$. Notice that the following inequalities,

$$\begin{aligned} \frac{dy_i}{dt} &= \frac{a_i x_i y_i}{1 + x_i} - d_i y_i + \rho_i (1 - s) \left(\frac{a_i x_i y_i}{1 + x_i} y_j \right) + \rho_i s (y_j - y_i) \\ &\geq \frac{a_i x_i y_i}{1 + x_i} - d_i y_i - \rho_i s y_i \Rightarrow \\ \frac{dy_i}{y_i dt} &\geq \frac{a_i x_i}{1 + x_i} - d_i - \rho_i s \end{aligned}$$

therefore, we have

$$\left. \frac{dy_i}{y_i dt} \right|_{E_{K_i, 00}} \geq \frac{a_i K_i}{1 + K_i} - (d_i + \rho_i s).$$

According to Theorem 2.5 of Hutson (1984) (Hutson, 1984), we can conclude that predator y_i is persistent if the following inequalities hold

$$\frac{a_i K_i}{1 + K_i} - (d_i + \rho_i s) > 0 \Leftrightarrow \rho_i s < \frac{(a_i - d_i)(K_i - \mu_i)}{1 + K_i}.$$

Now assume that $\rho_i s < \frac{(a_i - d_i)(K_i - \mu_i)}{1 + K_i}$ holds, then we can conclude that predator y_i is persistent. This implies that when time large enough, there exists some $\epsilon > 0$ such that

$$\left. \frac{dy_i}{dt} \right|_{y_i=0} = \rho_j s y_j > \rho_j s \epsilon > 0.$$

Thus, we could conclude that predator in Patch j also persists due to the persistence of predator in Patch i .

□

Proof of Proposition 3.1

Proof. The algebraic calculations imply that an interior equilibrium (x_i^*, y_i^*, y_j^*) of Model (3) satisfies the following equations:

$$\begin{aligned} y_i^* &= \frac{r_i(K_i - x_i^*)(1 + x_i^*)}{a_i K_i} \\ y_j^* &= \frac{r_i(K_i - x_i^*)[x_i^*(a_i - d_i) - d_i]\rho_j}{a_i K_i d_j \rho_i} \\ 0 &= \underbrace{[(x_i^*)^3 - (\mu_i + K_i)(x_i^*)^2 - \alpha_i x_i^* + \beta_i]}_{f_i(x_i^*)} [x_i^* + 1] \end{aligned}$$

where $\beta_i = \frac{[d_j \rho_i s + d_i(d_j + \rho_j s)]K_i}{r_i(a_i - d_i)(1 - s)\rho_j}$ and

$$\alpha_i = \frac{[d_j s \rho_i + r_i d_i(1 - s) - (a_i - d_i)(d_j + s \rho_j)]K_i}{r_i(a_i - d_i)(1 - s)\rho_j} = \beta_i + \frac{[r_i d_i(1 - s) - a_i(d_j + s \rho_j)]K_i}{r_i(a_i - d_i)(1 - s)\rho_j}.$$

This implies that

$$0 < \mu_i = \frac{d_i}{a_i - d_i} < x_i^* < K_i \text{ and } f_i(x_i^*) = 0.$$

Therefore, if $a_i < d_i$ or $\mu_i > K_i$ or $f_i(x_i^*) = 0$ has no positive roots, then Model (3) has no interior equilibrium.

Now assume that $0 < \mu_i = \frac{d_i}{a_i - d_i} < K_i$, then we have $f_i(0) = \beta_i > 0$ and $\lim_{x_i \rightarrow -\infty} f_i(x_i) = -\infty$. This indicates that there exist $x_0 \in (-\infty, 0)$ such that $f_i(x_0) = 0$. Therefore, we can conclude that $f_i(x_i)$ has at least one negative root and at most two positive roots since $f_i(x_i)$ is a polynomial with degree 3. The derivative of $f_i(x_i)$ has the following form

$$f_i'(x_i) = 3x_i^2 - 2(\mu_i + K_i)x_i - \alpha_i = 0$$

which gives the following two critical points if $\Delta_i = (\mu_i + K_i)^2 + 3\alpha_i > 0$

$$x_i^{c+, -} = \frac{(\mu_i + K_i) \pm \sqrt{(\mu_i + K_i)^2 + 3\alpha_i}}{3} = \frac{(\mu_i + K_i) \pm \sqrt{\Delta_i}}{3}.$$

Therefore if $\Delta_i \geq 0$, then $x_i^{c+} = \frac{(\mu_i + K_i) + \sqrt{\Delta_i}}{3} > 0$ is the local minimum of $f_i(x_i)$ since $f_i''(x_i^{c+}) = 2\sqrt{\Delta_i} \geq 0$ and $f_i''(x_i^{c-}) = -2\sqrt{\Delta_i} \leq 0$. We note that $f_i(x_i)$ has two positive roots if $f_i(x_i^{c+}) \leq 0$. It follows that $f_i(x_i)$ has two positive roots if the following equation is satisfied:

$$f(x_i^{c+}) = -\frac{1}{3}[\alpha_i(\mu_i + K_i) - 3\beta_i] - \frac{1}{27}[(\mu_i + K_i) + 3\alpha_i]^2 [2(\mu_i + K_i) - \sqrt{\Delta_i}] - \frac{1}{3}\alpha_i \sqrt{\Delta_i} < 0.$$

Since

$$\alpha_i(\mu_i + K_i) - 3\beta_i > 0 \quad \Rightarrow \quad \alpha_i > \frac{3\beta_i}{\mu_i + K_i}$$

and

$$2(\mu_i + K_i) - \sqrt{\Delta_i} = 2(\mu_i + K_i) - \sqrt{(\mu_i + K_i)^2 + 3\alpha_i} > 0 \Rightarrow \alpha_i < (\mu_i + K_i)^2$$

therefore we can conclude that $f_i(x_i)$ has two positive roots when $\frac{3\beta_i}{\mu_i + K_i} < \alpha_i < (\mu_i + K_i)^2$. Thus for $x_{i\ell}^*$ where $\ell = 1, 2$ denote the two positive roots of the nullclines $f_i(x_i)$ and $i = 1, 2$ represent the prey population in patch one and two, we have:

$$y_{i\ell}^* = \frac{(K_i - x_{i\ell}^*)(1 + x_{i\ell}^*)}{a_i K_i}, \quad y_{j\ell}^* = \frac{(K_i - x_{i\ell}^*)[x_{i\ell}^*(a_i - d_i) - d_i]\rho_j}{a_i K_i d_j \rho_i}$$

if $\mu_i < x_{i\ell}^* < K_i, \ell = 1, 2$.

From the arguments above we conclude that Model (3) can have up to two interior equilibria $E_{x_i, y_i, y_j}^\ell = (x_{i\ell}^*, y_{i\ell}^*, y_{j\ell}^*)$ when $\frac{3\beta_i}{\mu_i + K_i} < \alpha_i < (\mu_i + K_i)^2$ and $\mu_i < x_{i\ell}^* < K_i, \ell = 1, 2$.

On the other hand, if $\Delta_i = (\mu_i + K_i)^2 + 3\alpha_i < 0$ then $f_i(x_i)$ has no positive real roots and hence Model (3) has no interior equilibrium. \square

Proof of Theorem 3.2

Proof. The local stability of the equilibrium $(x_1^*, y_1^*, x_2^*, y_2^*)$ of Model (1) is established by finding the eigenvalues $\lambda_i, i = 1, 2, 3, 4$ of the Jacobian matrix $J_{(x_1^*, y_1^*, x_2^*, y_2^*)}$ (11) evaluated at the equilibria.

$$J_{(x_1^*, y_1^*, x_2^*, y_2^*)} = \begin{bmatrix} \left(1 - \frac{2x_1^*}{K_1}\right) - \frac{a_1 y_1^*}{(1+x_1^*)^2} & -\frac{a_1 x_1^*}{1+x_1^*} & 0 & 0 \\ \frac{a_1 y_1^* (1+y_2^* (\rho_1 - s\rho_1))}{(1+x_1^*)^2} & \rho_1 (1-s) \left(\frac{a_1 x_1^* y_2^*}{1+x_1^*} - \frac{a_2 x_2^* y_2^*}{1+x_2^*} \right) + \frac{a_1 x_1^*}{1+x_1^*} - d_1 - s\rho_1 & \frac{\rho_1 a_2 (-1+s) y_1^* y_2^*}{(1+x_2^*)^2} & s\rho_1 + \rho_1 (1-s) \left(\frac{a_1 x_1^* y_1^*}{1+x_1^*} - \frac{a_2 x_2^* y_1^*}{1+x_2^*} \right) \\ 0 & 0 & r \left(1 - \frac{2x_2^*}{K_2} \right) - \frac{a_2 y_2^*}{(1+x_2^*)^2} & -\frac{a_2 x_2^*}{1+x_2^*} \\ \frac{\rho_2 a_1 (-1+s) y_1^* y_2^*}{(1+x_2^*)^2} & s\rho_2 + \rho_2 (1-s) \left(\frac{a_2 x_2^* y_2^*}{1+x_2^*} - \frac{a_1 x_1^* y_1^*}{1+x_1^*} \right) & \frac{a_2 y_2^* (1+y_1^* (\rho_2 - s\rho_2))}{(1+x_2^*)^2} & \rho_2 (1-s) \left(\frac{a_2 x_2^* y_1^*}{1+x_2^*} - \frac{a_1 x_1^* y_1^*}{1+x_1^*} \right) + \frac{a_2 x_2^*}{1+x_2^*} - d_2 - s\rho_2 \end{bmatrix}$$

By substituting the equilibria $E_{0000}, E_{K_1 000}, E_{00 K_2 0}$, into the Jacobian matrix (11), it was found that these equilibria are saddle consider one of their eigenvalues is positive.

For the equilibrium $E_{K_1 0 K_2 0}$ we obtain

$$\lambda_1 = -1 (< 0), \quad \lambda_2 = -r (< 0),$$

$$\lambda_3 + \lambda_4 = \frac{a_1 K_1}{1 + K_1} - d_1 + \frac{a_2 K_2}{1 + K_2} - d_2 - s\rho_1 - s\rho_2$$

and

$$\lambda_3 \lambda_4 = \left[d_1 - \frac{a_1 K_1}{1 + K_1} \right] \left[1 - \frac{a_2 K_2}{(s\rho_2 + d_2)(1 + K_2)} \right] + \frac{s\rho_1}{s\rho_2 + d_2} \left[d_2 - \frac{a_2 K_2}{1 + K_2} \right]$$

Notice that the eigenvalue λ_3 and λ_4 being negative for $s \in (0, 1)$ is equivalent to the case where the boundary equilibria $(K_i, 0)$ for the single patch is globally asymptotically stable. This is also equivalent to $\mu_i > K_i$ or $\frac{a_i K_i}{1 + K_i} - d_i < 0$. We again observe that for $\frac{a_i K_i}{1 + K_i} - d_i < 0$ the following holds

$$\lambda_3 + \lambda_4 = \frac{a_1 K_1}{1 + K_1} - d_1 + \frac{a_2 K_2}{1 + K_2} - d_2 - s\rho_1 - s\rho_2 < 0 \Rightarrow d_1 + d_2 + s\rho_1 + s\rho_2 > \frac{a_1 K_1}{1 + K_1} + \frac{a_2 K_2}{1 + K_2}$$

and

$$\lambda_3 \lambda_4 = \left[d_1 - \frac{a_1 K_1}{1 + K_1} \right] \left[1 - \frac{a_2 K_2}{(s \rho_2 + d_2)(1 + K_2)} \right] + \frac{s \rho_1}{s \rho_2 + d_2} \left[d_2 - \frac{a_2 K_2}{1 + K_2} \right] > 0$$

which can be rewritten in the following form:

$$\sum_{i=1}^2 \left[\frac{(a_i - d_i)(\mu_i - K_i)}{1 + K_i} + s \rho_i \right] > 0$$

and

$$\left[\frac{(a_1 - d_1)(\mu_1 - K_1)}{1 + K_1} \right] \left[s \rho_2 + \frac{(a_2 - d_2)(\mu_2 - K_2)}{1 + K_2} \right] + s \rho_1 \left[\frac{(a_2 - d_2)(\mu_2 - K_2)}{1 + K_2} \right] > 0.$$

Based on the discussion above, we can conclude that the results on the local stability of four boundary equilibria of Theorem 3.2 holds.

Item 1: Let $p_i(x) = \frac{a_i x}{1+x}$ and $q_i(x) = \frac{r_i(K_i-x)(1+x)}{a_i K_i}$ then we have the following

$$\frac{dx_i}{dt} = r_i x_i \left(1 - \frac{x_i}{K_i} \right) - \frac{a_i x_i y_i}{(1+x_i)} = \frac{a_i x_i}{1+x_i} \left[\frac{r_i(K_i-x_i)(1+x_i)}{a_i K_i} - y_i \right] = p_i(x_i) [q_i(x_i) - y_i].$$

$$\frac{dy_i}{dt} = y_i \left[\frac{a_i x_i}{1+x_i} - d_i \right] + \rho_i (1-s) y_i y_j \left[\frac{a_i x_i}{1+x_i} - \frac{a_j x_j}{1+x_j} \right] + \rho_i s [y_j - y_i]$$

$$= y_i [p_i(x_i) - d_i] + \rho_i (1-s) y_i y_j [p_i(x_i) - p_j(x_j)] + \rho_i s [y_j - y_i] \text{ where both } i, j = 1, 2, \text{ with } i \neq j$$

Now consider the following Lyapunov functions

$$V_1(x_1, y_1) = \rho_2 \int_{K_1}^{x_1} \frac{p_1(\xi) - p_1(K_1)}{p_1(\xi)} d\xi + \rho_2 y_1 \quad (12)$$

and

$$V_2(x_2, y_2) = \rho_1 \int_{K_2}^{x_2} \frac{p_2(\xi) - p_2(K_2)}{p_2(\xi)} d\xi + \rho_1 y_2 \quad (13)$$

Taking derivative of the functions (12) and (13) with respect to time t yield

$$\begin{aligned} \frac{d}{dt} V_1(x_1(t), y_1(t)) &= \rho_2 \frac{p_1(x_1) - p_1(K_1)}{p_1(x_1)} \frac{dx_1}{dt} + \rho_2 \frac{dy_1}{dt} \\ &= \rho_2 \frac{1}{p_1(x_1)} [p_1(x_1) - p_1(K_1)] p_1(x_1) [q_1(x_1) - y_1] + \rho_2 y_1 [p_1(x_1) - d_1] + \rho_1 \rho_2 (1-s) y_1 y_2 [p_1(x_1) - p_2(x_2)] \\ &\quad + \rho_1 \rho_2 s [y_2 - y_1] \\ &= \rho_2 [p_1(x_1) - p_1(K_1)] q_1(x_1) + \rho_2 y_1 [p_1(K_1) - d_1] + \rho_1 \rho_2 (1-s) y_1 y_2 [p_1(x_1) - p_2(x_2)] + \rho_1 \rho_2 s [y_2 - y_1] \end{aligned} \quad (14)$$

and

$$\begin{aligned} \frac{d}{dt} V_2(x_2(t), y_2(t)) &= \rho_1 \frac{p_2(x_2) - p_2(K_2)}{p_2(x_2)} \frac{dx_2}{dt} + \rho_1 \frac{dy_2}{dt} \\ &= \rho_1 \frac{1}{p_2(x_2)} [p_2(x_2) - p_2(K_2)] p_2(x_2) [q_2(x_2) - y_2] + \rho_1 y_2 [p_2(x_2) - d_2] + \rho_1 \rho_2 (1-s) y_1 y_2 [p_2(x_2) - p_1(x_1)] \\ &\quad + \rho_1 \rho_2 s [y_1 - y_2] \\ &= \rho_1 [p_2(x_2) - p_2(K_2)] q_2(x_2) + \rho_1 y_2 [p_2(K_2) - d_2] - \rho_1 \rho_2 (1-s) y_1 y_2 [p_1(x_1) - p_2(x_2)] - \rho_1 \rho_2 s [y_2 - y_1] \end{aligned} \quad (15)$$

Also, we denote $V = V_1 + V_2$ and adding (14) and (15), we obtain

$$\begin{aligned}\frac{d}{dt}V &= \frac{d}{dt}V_1(x_1(t), y_1(t)) + \frac{d}{dt}V_2(x_2(t), y_2(t)) \\ &= \rho_2 [p_1(x_1) - p_1(K_1)] [q_1(x_1) - y_1] + \rho_2 y_1 [p_1(x_1) - d_1] + \rho_1 [p_2(x_2) - p_2(K_2)] [q_2(x_2) - y_2] + \rho_1 y_2 [p_2(x_2) - d_2] \\ &= \rho_2 [p_1(x_1) - p_1(K_1)] q_1(x_1) + \rho_2 y_1 [p_1(K_1) - d_1] + \rho_1 [p_2(x_2) - p_2(K_2)] q_2(x_2) + \rho_1 y_2 [p_2(K_2) - d_2].\end{aligned}$$

We observe that the function $p_i(x_i)$ increases as x_i increases thus $p_i(x_i) - p_i(K_i) > 0$ if $x_i > K_i$ and $p_i(x_i) - p_i(K_i) < 0$ if $x_i < K_i$. Also, $q_i(x_i)$ is positive if $x_i < K_i$ and it is negative if $x_i > K_i$. This implies that the expressions $\rho_2 [p_1(x_1) - p_1(K_1)] q_1(x_1)$ and $\rho_1 [p_2(x_2) - p_2(K_2)] q_2(x_2)$ are both negative for all $x_i \geq 0$ since all the parameters are assumed to be positive. Also, Assume $\mu_i > K_i$. This implies that $\frac{d_i}{a_i - d_i} > K_i$ which is also equivalent to $\frac{a_i K_i}{1 + K_i} = p_i(K_i) < d_i$. Since $p_i(K_i) < d_i$ then $p_i(K_i) - d_i < 0$. The derivative $\frac{dV}{dt}$ is therefore negative which implies that both V_1 and V_2 are Lyapunov functions, and the boundary equilibrium $E_{K_1 0 K_2 0} = (K_1, 0, K_2, 0)$ is globally stable when $\mu_i > K_i$ by Theorem 3.2 in Hsu (1978).

Item 2: According to Theorem 2.1, we know that Model (1) is attracted to a compact set C in \mathbb{R}_+^4 . Define $V_x = x_1 + x_2$, then we have

$$\frac{dV_x}{dt} = \frac{dx_1}{dt} + \frac{dx_2}{dt} = r_1 x_1 \left(1 - \frac{x_1}{K_1}\right) - \frac{a_1 x_1 y_1}{1 + x_1} + r_2 x_2 \left(1 - \frac{x_2}{K_2}\right) - \frac{a_2 x_2 y_2}{1 + x_2}.$$

Notice that if $x_i = x_j = 0$, then Model (1) converges to $(0, 0, 0, 0)$, and

$$\left. \frac{dV_x}{dt} \right|_{x_1=x_2=0} = r_1 + r_2 > 0.$$

Therefore, according to Theorem 2.5 of Hutson (1984), we can conclude that prey population in two patches, i.e., $x_1 + x_2$, is persistent. Moreover, if $x_j = 0$, Model (1) is reduced to the subsystem (3) where prey x_i is persistent according to Theorem 3.1. Thus, we can conclude prey population in at least one patch is persistent.

Define $V_y = \rho_2 y_1 + \rho_1 y_2$, then we have

$$\frac{dV_y}{dt} = \rho_2 \frac{dy_1}{dt} + \rho_1 \frac{dy_2}{dt} = \rho_2 y_1 \left(\frac{a_1 x_1}{1 + x_1} - d_1 \right) + \rho_1 y_2 \left(\frac{a_2 x_2}{1 + x_2} - d_2 \right).$$

Notice that if $y_i = y_j = 0$, then Model (1) converges to $(K_1, 0, K_2, 0)$. Since we have $K_i > \mu_i$ for both $i = 1, 2$, then we have

$$\min_{i=1,2} \left\{ \frac{a_i K_i}{1 + K_i} - d_i \right\} = \delta > 0.$$

This implies that

$$\left. \frac{dV_y}{dt} \right|_{y_1=y_2=0} = \rho_2 y_1 \left(\frac{a_1 K_1}{1 + K_1} - d_1 \right) + \rho_1 y_2 \left(\frac{a_2 K_2}{1 + K_2} - d_2 \right) \geq \delta (\rho_2 y_1 + \rho_1 y_2) = \delta V_y > 0.$$

Therefore, according to Theorem 2.5 of Hutson (1984) and the proof of Proposition 3.1, we can conclude that predator population in each patch is persistent.

□

Proof of Theorem 3.3

Proof. First we show the existence of the interior equilibrium $E = (\mu, \nu, \mu, \nu)$ in the symmetric case (i.e. $a_1 = a_2 = a, d_1 = d_2 = d, K_1 = K_2 = K, r = 1$). The interior equilibrium can be obtained by the positive intersection of the two nullclines $x_1 = F_1(x_2)$ and $x_2 = F_2(x_1)$ (10). Recall from the nullclines (10) that

$$x_i(x_j) = \frac{(\mu + K) \pm \sqrt{(\mu + K)^2 - 4\phi_i(x_j)}}{2}.$$

where $\phi_i(x_j) = \mu K + \frac{\rho_i}{\rho_j}(x_j - \mu)(x_j - K)$ which indicate that

$$x_i^+(\mu) = \frac{(\mu + K) + \sqrt{(\mu + K)^2 - 4\phi_i(\mu)}}{2} = K \text{ and } x_i^-(\mu) = \frac{(\mu + K) - \sqrt{(\mu + K)^2 - 4\phi_i(\mu)}}{2} = \mu$$

This implies that $x = \mu$ is a positive solution of the nullcline (10) when $a > d$ in the symmetric case. We can accordingly say that $E = (\mu, \nu, \mu, \nu)$ is an interior equilibrium of Model (1) when $a_1 = a_2 = a, d_1 = d_2 = d, K_1 = K_2 = K, r = 1$.

The local stability of $E = (\mu, \nu, \mu, \nu)$ is obtained by the eigenvalues of the Jacobian matrix (11) evaluated at this equilibrium as follow:

$$\begin{aligned} \lambda_1 \lambda_2 &= \frac{d(K - \mu)}{K(1 + \mu)} > 0 \text{ if } K > \mu \text{ and } \lambda_1 \lambda_2 = \frac{d(K - \mu)}{K(1 + \mu)} < 0 \text{ if } K < \mu \\ \lambda_1 + \lambda_2 &= \frac{K - 1 - 2\mu}{K(1 + \mu)} < 0 \text{ if } \mu > \frac{K - 1}{2} \text{ and } \lambda_1 + \lambda_2 = \frac{d(K - \mu)}{K(1 + \mu)} > 0 \text{ if } \mu < \frac{K - 1}{2} \\ \lambda_3 \lambda_4 &= \frac{(\rho_1 + \rho_2)[(1 - s)(K - \mu)d\nu - ((K - 1) - 2\mu)s\mu] + d(K - \mu)}{K(1 + \mu)} > 0 \text{ for } K > \mu \text{ and } \mu > \frac{K - 1}{2} \text{ when } s \in [0, 1] \\ \lambda_3 + \lambda_4 &= - \left[\frac{-\mu(K - 1) + 2\mu^2 + Ks(\rho_1 + \rho_2)(1 + \mu)}{K(1 + \mu)} \right] < 0 \text{ for } \mu > \frac{K - 1}{2} \text{ when } s \in [0, 1] \end{aligned}$$

Notice that the eigenvalues $\lambda_1, \lambda_2, \lambda_3,$ and λ_4 being negative correspond to the case where the unique interior equilibrium (μ, ν) of the single patch Model (2) is locally asymptotically stable. We can hence conclude that E has the same local stability as the interior equilibrium (μ, ν) for the single patch model (2). Consequently $\frac{K-1}{2} < \mu < K$ are sufficient conditions for $E = (\mu, \nu, \mu, \nu)$ to be locally asymptotically stable while unstable when $\mu < \frac{K-1}{2}$ for $s \in [0, 1]$.

□

Acknowledgement

This research of Y.K. is partially supported by NSF-DMS (1313312). The research of K.M is partially supported by the Department of Education GAANN (P200A120192). We would like to give a special appreciation to Marisabel Rodriguez and Daniel Burkow for their assistances.

References

Alonso, J. C., Martín, C. A., Alonso, J. A., Palacín, C., Magaña, M., and Lane, S. J. (2004). Distribution dynamics of a great bustard metapopulation throughout a decade: influence of conspecific attraction and recruitment. *Biodiversity & Conservation*, 13(9):1659–1674.

- Auger, P. and Poggiale, J.-C. (1996). Emergence of population growth models: fast migration and slow growth. *Journal of Theoretical Biology*, 182(2):99–108.
- Bowler, D. E. and Benton, T. G. (2005). Causes and consequences of animal dispersal strategies: relating individual behaviour to spatial dynamics. *Biological Reviews*, 80(02):205–225.
- Clobert, J., Danchin, E., Dhondt, A. A., and Nichols, J. D. (2001). *Dispersal*. Oxford University Press Oxford.
- Cressman, R. and Krivan, V. (2013). Two-patch population models with adaptive dispersal: the effects of varying dispersal speeds. *Journal of mathematical biology*, 67(2):329–358.
- Fraser, D. F. and Cerri, R. D. (1982). Experimental evaluation of predator-prey relationships in a patchy environment: consequences for habitat use patterns in minnows. *Ecology*, pages 307–313.
- Ghosh, S. and Bhattacharyya, S. (2011). A two-patch prey-predator model with food-gathering activity. *Journal of Applied Mathematics and Computing*, 37(1-2):497–521.
- Gilpin, M. and Hanski, I. (1991). *Metapopulation dynamics: brief history and conceptual domain*. Academic Press, London.
- Hanski, I. (1999). Habitat connectivity, habitat continuity, and metapopulations in dynamic landscapes. *Oikos*, pages 209–219.
- Hansson, L. (1991). Dispersal and connectivity in metapopulations. *Biological journal of the Linnean Society*, 42(1-2):89–103.
- Hassell, M. and Southwood, T. (1978). Foraging strategies of insects. *Annual Review of Ecology and Systematics*, pages 75–98.
- Hastings, A. (1983). Can spatial variation alone lead to selection for dispersal? *Theoretical Population Biology*, 24(3):244–251.
- Hsu, S., Hubbell, S., and Waltman, P. (1977). A mathematical theory for single-nutrient competition in continuous cultures of micro-organisms. *SIAM Journal on Applied Mathematics*, 32(2):366–383.
- Hsu, S.-B. (1978). On global stability of a predator-prey system. *Mathematical Biosciences*, 39(1):1–10.
- Huang, Y. and Diekmann, O. (2001). Predator migration in response to prey density: what are the consequences? *Journal of mathematical biology*, 43(6):561–581.
- Hutson, V. (1984). A theorem on average liapunov functions. *Monatshefte für Mathematik*, 98(4):267–275.
- Ims, R. A. and Hjermann, D. (2001). Condition-dependent dispersal. *Dispersal*. Oxford University Press, Oxford, pages 203–216.
- Jánosi, I. M. and Scheuring, I. (1997). On the evolution of density dependent dispersal in a spatially structured population model. *Journal of Theoretical Biology*, 187(3):397–408.
- Jansen, V. A. (1995). Regulation of predator-prey systems through spatial interactions: a possible solution to the paradox of enrichment. *Oikos*, 74(345):384–390.
- Jansen, V. A. (2001). The dynamics of two diffusively coupled predator-prey populations. *Theoretical Population Biology*, 59(2):119–131.
- Kang, Y., Sasmal, S. K., and Messan, K. (2014). A two-patch prey-predator model with dispersal in predators driven by the strength of predation. *Submitted to the Journal of Mathematical Biology*.

- Kareiva, P. and Odell, G. (1987). Swarms of predators exhibit "preytaxis" if individual predators use area-restricted search. *American Naturalist*, 130(2):233–270.
- Kiester, A. and Slatkin, M. (1974). A strategy of movement and resource utilization. *Theoretical population biology*, 6(1):1–20.
- Kummel, M., Brown, D., and Bruder, A. (2013). How the aphids got their spots: predation drives self-organization of aphid colonies in a patchy habitat. *Oikos*, 122(6):896–906.
- Liu, X. and Chen, L. (2003). Complex dynamics of holling type ii lotka–volterra predator–prey system with impulsive perturbations on the predator. *Chaos, Solitons & Fractals*, 16(2):311–320.
- Markin, G. P. (1970). Foraging behavior of the argentine ant in a california citrus grove. *Journal of Economic Entomology*, 63(3):740–744.
- Massot, M., Clobert, J., Lorenzon, P., and Rossi, J.-M. (2002). Condition-dependent dispersal and ontogeny of the dispersal behaviour: an experimental approach. *Journal of Animal Ecology*, 71(2):253–261.
- Matthysen, E. (2005). Density-dependent dispersal in birds and mammals. *Ecography*, 28(3):403–416.
- Namba, T. (1980). Density-dependent dispersal and spatial distribution of a population. *Journal of theoretical biology*, 86(2):351–363.
- Nguyen-Ngoc, D., Nguyen-Huu, T., and Auger, P. (2012). Effects of fast density dependent dispersal on pre-emptive competition dynamics. *Ecological Complexity*, 10:26–33.
- Poggiale, J. (1998). From behavioural to population level: growth and competition. *Mathematical and computer modelling*, 27(4):41–49.
- Ronce, O., Olivieri, I., Clobert, J., Danchin, E. G., et al. (2001). Perspectives on the study of dispersal evolution. *Dispersal*, pages 341–357.
- Rosenzweig, M. L. and MacArthur, R. H. (1963). Graphical representation and stability conditions of predator-prey interactions. *American Naturalist*, 97(895):209–223.
- Savino, J. F. and Stein, R. A. (1989). Behavioural interactions between fish predators and their prey: effects of plant density. *Animal behaviour*, 37:311–321.
- Silva, J. A., De Castro, M. L., and Justo, D. A. (2001). Stability in a metapopulation model with density-dependent dispersal. *Bulletin of mathematical biology*, 63(3):485–505.
- Stamps, J. (1988). Conspecific attraction and aggregation in territorial species. *American Naturalist*, pages 329–347.
- Taylor, F. (1977). Foraging behavior of ants: experiments with two species of myrmecine ants. *Behavioral Ecology and Sociobiology*, 2(2):147–167.
- Thieme, H. R. (2003). *Mathematics in population biology*. Princeton University Press.
- Traniello, J. F., Fujita, M. S., and Bowen, R. V. (1984). Ant foraging behavior: ambient temperature influences prey selection. *Behavioral Ecology and Sociobiology*, 15(1):65–68.